NAVAL POSTGRADUATE SCHOOL
Monterey, California

THESIS

Mixed and Forced Convection from an Array
of Discrete Heat Sources in a
Vertical Channel

by

James D. Syring

March, 1992

Thesis Advisor: Y.K. Joshi

Approved for public release; distribution is unlimited.

T258712

REPORT DOCUMENTATION PAGE

Form Approved
OMB No 0704-0188

1a REPORT SECURITY CLASSIFICATION Unclassified	1b RESTRICTIVE MARKINGS
2a SECURITY CLASSIFICATION AUTHORITY	3 DISTRIBUTION / AVAILABILITY OF REPORT Approved for public release: Distribution is unlimited
2b DECLASSIFICATION / DOWNGRADING SCHEDULE	
4 PERFORMING ORGANIZATION REPORT NUMBER(S)	5 MONITORING ORGANIZATION REPORT NUMBER(S)
6a NAME OF PERFORMING ORGANIZATION Naval Postgraduate School 6b OFFICE SYMBOL (If applicable) ME	7a NAME OF MONITORING ORGANIZATION Naval Postgraduate School
6c ADDRESS (City, State, and ZIP Code) Monterey, CA 93943-5000	7b ADDRESS (City, State, and ZIP Code) Monterey, CA 93943-5000
8a NAME OF FUNDING / SPONSORING ORGANIZATION 8b OFFICE SYMBOL (If applicable)	9 PROCUREMENT INSTRUMENT IDENTIFICATION NUMBER
8c ADDRESS (City, State, and ZIP Code)	10 SOURCE OF FUNDING NUMBERS PROGRAM ELEMENT NO / PROJECT NO / TASK NO / WORK UNIT ACCESSION NO

11 TITLE (Include Security Classification)
MIXED AND FORCED CONVECTION FROM AN ARRAY OF DISCRETE HEAT SOURCES IN A VERTICAL CONVECTION

12 PERSONAL AUTHOR(S)
James D. Syring

13a TYPE OF REPORT	13b TIME COVERED	14 DATE OF REPORT (Year, Month, Day)	15 PAGE COUNT
Master's Thesis	FROM _____ TO _____	MARCH 1992	89

16 SUPPLEMENTARY NOTATION
The views expressed are those of the author and do not reflect the official policy or position of the Department of Defense or the U.S. Government

17 COSATI CODES		
FIELD	GROUP	SUB-GROUP

18 SUBJECT TERMS (Continue on reverse if necessary and identify by block number)
pulsatile flow, opposed mixed convection, temperature variation

19 ABSTRACT (Continue on reverse if necessary and identify by block number)

Mixed and forced convection liquid cooling of discrete heat sources in a vertical channel was investigated. Ten heat sources were flush mounted to one of the plexiglass channel walls, while the opposite wall was insulated. Measurements of heater surface temperatures were made for a channel Reynolds number range of 500-7300 and heat flux range of 510-2700 W/m^2. Temperature patterns on the heated surface were visualized using liquid crystals. Effects of flow pulsations were also investigated in the 0-1.25 Hz range.

20 DISTRIBUTION / AVAILABILITY OF ABSTRACT	21 ABSTRACT SECURITY CLASSIFICATION
☒ UNCLASSIFIED/UNLIMITED ☐ SAME AS RPT ☐ DTIC USERS	Unclassified
22a NAME OF RESPONSIBLE INDIVIDUAL Yogendra Joshi	22b TELEPHONE (Include Area Code) 646-3400 22c OFFICE SYMBOL ME/Jo

Approved for public release; distribution is unlimited.

Mixed and Forced Convection from an Array
of Discrete Heat Sources in a Vertical Channel

by

James D. Syring
Lieutenant, United States Navy
B.S., United States Naval Academy, 1985

Submitted in partial fulfillment
of the requirements for the degree of

MASTER OF SCIENCE IN MECHANICAL ENGINEERING

from the

NAVAL POSTGRADUATE SCHOOL
March 1992

ABSTRACT

Mixed and forced convection liquid cooling of discrete heat sources in a vertical channel was investigated. Ten heat sources were flush mounted to one of the plexiglass channel walls, while the opposite wall was insulated. Measurements of heater surface temperatures were made for a channel Reynolds number range of 500-7300 and heat flux range of 510-2700 W/m^2 . Temperature patterns on the heated surface were visualized using liquid crystals. Effects of flow pulsations on heat transfer were also investigated in the 0-1.25 Hz range.

C.1

TABLE OF CONTENTS

I. INTRODUCTION 1

A. ELECTRONIC COOLING 1

B. PREVIOUS RESEARCH IN PULSATILE FLOW 3

C. MIXED CONVECTION RESEARCH 5

D. OBJECTIVES 7

II. EXPERIMENTAL APPARATUS 9

A. TEST CHANNEL ASSEMBLY 9

1. Vertical Channel 9

2. Power Distribution System 17

3. Data Acquisition Assembly 17

B. LIQUID CRYSTALS 19

C. EXPERIMENTAL PROCEDURE 19

III. RESULTS 22

A. DATA ANALYSIS 22

B. PULSATILE FLOW RESULTS 25

C. MIXED CONVECTION RESULTS (NO VANE ROTATION) . . 36

1. Results under nominally steady conditions . 38

2. Transient Results 55

D. LIQUID CRYSTAL RESULTS 69

IV. CONCLUSIONS 72

V. RECOMMENDATIONS 74

APPENDIX A 75

APPENDIX B 77

LIST OF REFERENCES 79

INITIAL DISTRIBUTION LIST 82

I. INTRODUCTION

A. ELECTRONIC COOLING

First generation computers, such as ENIAC, used vacuum tubes as the basic logic device. These computers were very massive and extremely slow and all were forced air cooled. With the invention of the transistor in 1947, engineers were driven to put more and more transistors on a circuit board in order to enhance machine performance. The trend has been of high packaging densities in the least amount of space. In addition, circuit power has been drastically increased in order to achieve higher circuit speed. All of these rapid advances in technology have caused the packaging engineer to search for more efficient methods of cooling these electronic circuits. Generally, junction temperatures of electronic components must be kept below $85^{\circ}C$. [Ref 1: pp.109-110] The reliability of electronic devices is markedly reduced for temperatures above this limit. Three methods of cooling electronic components will be discussed in the following; air cooling, conduction cooling and liquid immersion cooling.

Air cooling is by far the most common method of thermal control for electronic equipment. Natural convection air cooling can be used in low power and low packaging densities; however, for most electronic cooling applications in today's world, forced air cooling is necessary. Air cooled modules are generally used which may employ boundary layer flow, channel flow or impingement. There are several methods available to further enhance the heat transfer capability of air cooling. The addition of turbulators has been shown to increase the heat transfer coefficient by at least 42%. [Ref 2: p. 296]

In many of today's machines, packaging densities and heat fluxes have reached levels that air cooling is no longer sufficient. It has become necessary to develop conduction cooling modules. An example is the Thermal Conduction Module developed by IBM. [Ref 2: p. 296] This particular module has approximately 100 microchips which are mounted on a ceramic substrate with a spring loaded piston mounted above each chip which allows for varying chip height. A water cooled aluminum plate is mounted above each module to provide the primary path for heat escape. Conduction resistance between the chip and the cold plate proves to be the limiting factor in this method of electronic cooling. Improvements in this method include reducing the thermal path resistance and the use of thermal filler materials across physical gaps in the module.

Direct liquid cooling has recently received increased attention because of the extremely high heat transfer rates which are attainable. Different cooling methods employing liquids include natural convection, forced convection, phase change, jet impingement, free falling liquid films and the use of heat pipes [Ref 2: pp.300-302]. It has been suggested that the use of pulsatile flow may further enhance the cooling effectiveness of these methods. [Ref. 3]

B. PREVIOUS RESEARCH IN PULSATILE FLOW

Previous research on heat transfer in oscillatory flow is very contradictory in nature. Some studies indicate that oscillations may increase heat transfer coefficients in certain Reynolds number ranges. Other studies indicate that oscillations can decrease heat transfer at certain frequencies and Reynolds numbers. [Ref 3]

When considering oscillatory flow it is necessary to define a "quasi-steady" or "quasi-stationary" state. In the quasi-steady state, steady state correlations hold since the frequency of oscillations is low. Integration is carried out over time in order to determine an average heat transfer coefficient. The frequency region for which quasi-steady state relationships hold is well below 20 cycles/second. [Ref 3: p.172]

In 1961 Lemlich found that raising the frequency of oscillations above a critical value increased the heat

transfer coefficient, with each cycle acting as a small disturbance and exhibiting a mixing effect on the boundary layers involved. However, Lemlich also observed that under certain conditions the heat transfer coefficient decreased with an elevation in frequency due to cyclic fluctuations in wall temperatures. Lemlich observed that the effect of oscillations was more pronounced at low Reynolds numbers than at high and for natural convection than for forced convection for a fixed frequency and fixed amplitude. Experiments were conducted using a double pipe heat exchanger with flow oscillations produced by rapidly opening and closing a solenoid valve. The pulsations increased the overall heat transfer coefficient by 80% for a Reynolds number of 2000.[Ref 3: p. 173]

Azar analyzed the effect of forced oscillation of a fluid entering an electronic circuit pack channel. The experimental set-up consisted of two epoxy boards forming a channel, each containing nine simulated electronic components. Both natural and forced convection cooling were considered. The fluid was oscillated at low frequencies prior to entering the channel. It was discovered that forced oscillation enhanced cooling by as much as 15%. Natural convection actually degraded cooling in all cases.[Ref.4]

Perkins, Stephanoff and Murray studied mixing enhancement in flow as a result of periodically pulsed fluid motion in a channel containing protruding blocks. They found that

superimposing a periodic component on steady mainstream flow promotes noticeable cavity interaction with the mainstream flow. The fluid trapped within the cavity has a tendency to accelerate and decelerate; thus, creating large local velocity disturbances which have a beneficial effect on heat transfer rates within the cavities.[Ref.5]

Ludlow, Kirwan and Gainer studied the frequency dependence of heat transfer coefficients for water flowing through a tube. The experimental apparatus consisted of a double pipe heat exchanger in which flow in the center pipe was pulsed at frequencies from 10 to 160 cycles per minute in Reynolds numbers ranges between 3700 to 21,400. They discovered that pulsing can increase heat transfer coefficients by a factor of 5 with the greatest increases reported in Reynolds regimes in the transition from laminar to turbulent flow.[Ref.6]

Siegel and Perlmutter analyzed heat transfer for pulsating flow between parallel plates. They found that for high frequency and high pressure oscillations the results of velocity changes were small. For constant wall temperature or constant wall heat flux cases, they discovered that the results approach that of the quasi-steady solution for low frequency ranges.

C. MIXED CONVECTION RESEARCH

In many applications involving convective heat transfer both the natural and forced convection modes may be important.

An important issue is to be able to assess the relative importance of the two effects. In some applications, flow rates may be so low that forced convection can be neglected and natural convection effects dominate. In some situations the two effects may be of equal importance. This type of transport is commonly called mixed convection. This mode arises in several applications; cooling electronic circuitry by a fan, externally imposed flow in heated channels, hot wire/film anemometery in low velocity fields, vertical circular tube flows used in heat exchangers and nuclear technology. [Ref.7]

Mixed convection effects are governed by the non-dimensional group Gr/Re^n , where the Grashof number and Reynolds number represent respectively the vigor of natural and forced convection effects and n depends on boundary conditions, geometry, and fluid. As Gr/Re^n approaches zero, forced convection effects become dominant. As Gr/Re^n approaches infinity, natural convection effects are dominant. [Ref. 7] Most of the work in internal mixed convection has been limited to flows in vertical circular tubes due to its application to heat exchangers and nuclear technology. Almost all of the experimentation has been to

determine overall heat transfer rates with little attention given to temperature and velocity field descriptions.

Mixed convection flows can be further classified into aiding or opposing depending upon the direction of the buoyancy force relative to the forced flow. Most effort so far has concentrated on aiding flows due to their relative simplicity. In opposed flows instabilities and transition to turbulence may arise.

D. OBJECTIVES

The present study consisted of two parts. The first part investigated the effect of flow pulsations on overall heat transfer rates in a vertical discretely heated channel. During the course of the experimentation, it was discovered that at low Reynolds numbers substantial opposed mixed convection effects were present. Extensive surface temperature measurements were made for these conditions to understand these effects. These experiments formed the second part of this investigation.

The objectives were:

- To design and build a vertical channel in order to study flows in a large range of Reynolds numbers (500-7300).

- To study the effects of imposed periodic flow pulsations (0 to 1.25 Hz) on overall heat transfer rates in a vertical channel.

- To investigate mixed convection effects in a vertical channel and their influence on the surface temperature field distribution and overall heat transfer rates.

II. EXPERIMENTAL APPARATUS

A. TEST CHANNEL ASSEMBLY

As shown in Figure 1, the experimental apparatus consisted of three main assemblies; a vertical channel with one wall containing ten flush heaters, power distribution system to the heaters, and a data acquisition system.

1. Vertical Channel

The vertical channel consisted of two 1 cm thick plexiglass boards 2.0 m by 0.25 m separated by a 1 cm thick plexiglass spacer with a 2.5 cm wide and 1 mm thick gasket. The fluid employed was water which entered the top of the channel into a surge tank and was then forced down through the channel by a combination of gravity and the pressure gradient created by the centrifugal pump recirculating the fluid. After passing through a 5 cm flow straightening zone the fluid entered the test section. A rotating vane downstream from the test section produced the flow oscillations.

As shown in Figure 2, the rotating vane is a 9.0 mm diameter shaft with parallel flats machined to provide a

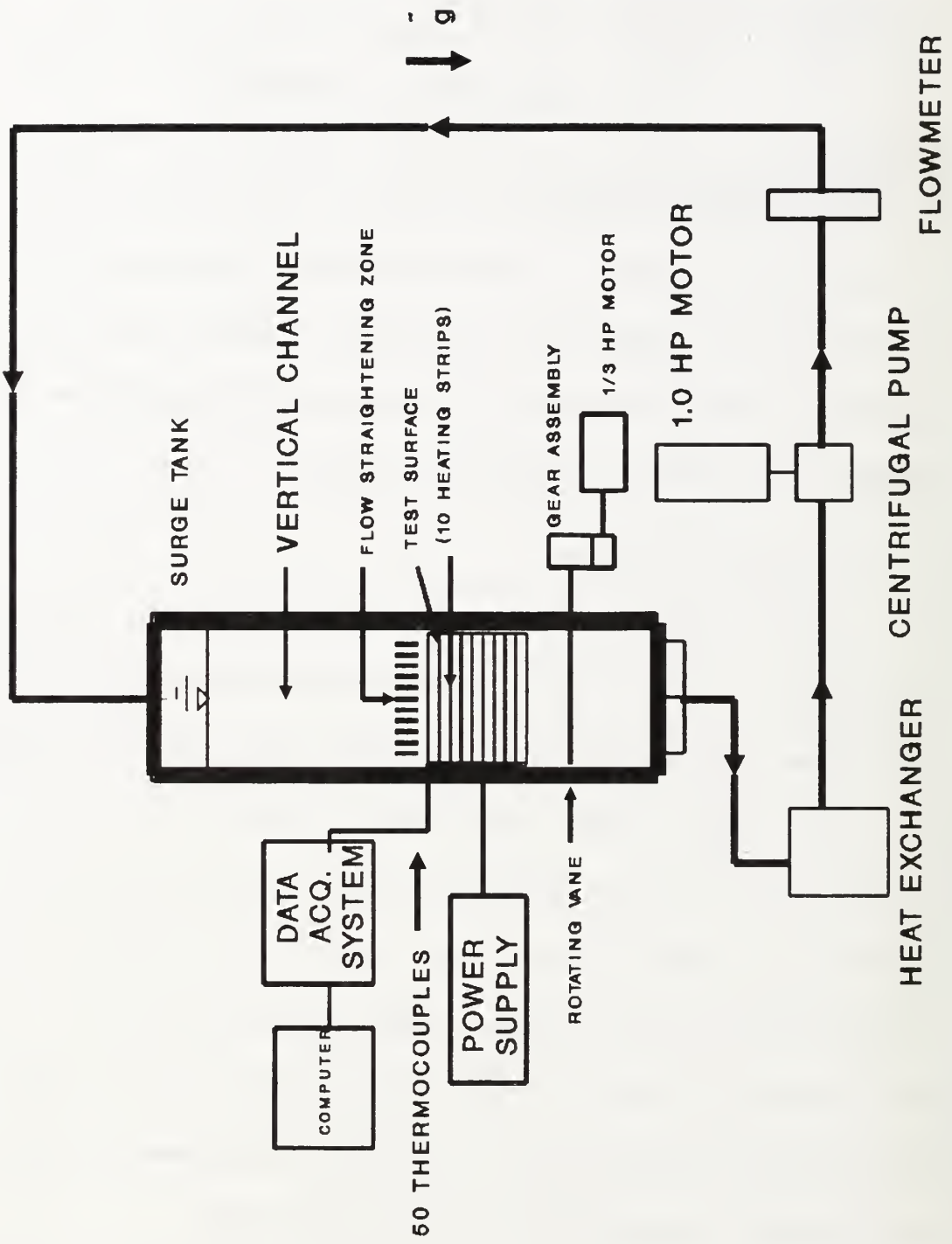

Figure 1. Overall schematic of experimental apparatus.

smaller cross section of 3.0 mm. The shaft is supported on roller bearings with exterior seals. An optical tachometer is used to accurately determine vane oscillation frequencies which could be varied from 0 to 75 RPM.

A Cole-Parmer positive displacement gear type pump driven by a variable speed motor produces Reynolds numbers of 500 (±50) to 15,000 (±10). Teflon fittings and tubing provide flow connections. An Omega turbine flowmeter monitors the flow rate. The flowmeter was calibrated in the Re range 500-4000 by weighing quantities of discharged water over specified times.

A heat exchanger was installed upstream of the pump in order to remove the bulk of the power dissipation from the heaters. The fluid temperature in the channel upstream of the test section was maintained constant within $0.1^{\circ}C$.

The test surface constituted one wall of the vertical channel. Ten 0.120 cm deep parallel grooves were milled horizontally across the test surface at spacings of 1 cm. These grooves served as thermocouple beds for each heating strip. A second, wider but shallower 1 cm thick and 0.08 cm deep groove, was milled on top of each of the thermocouple

REPRODUCED AT GOVERNMENT EXPENSE

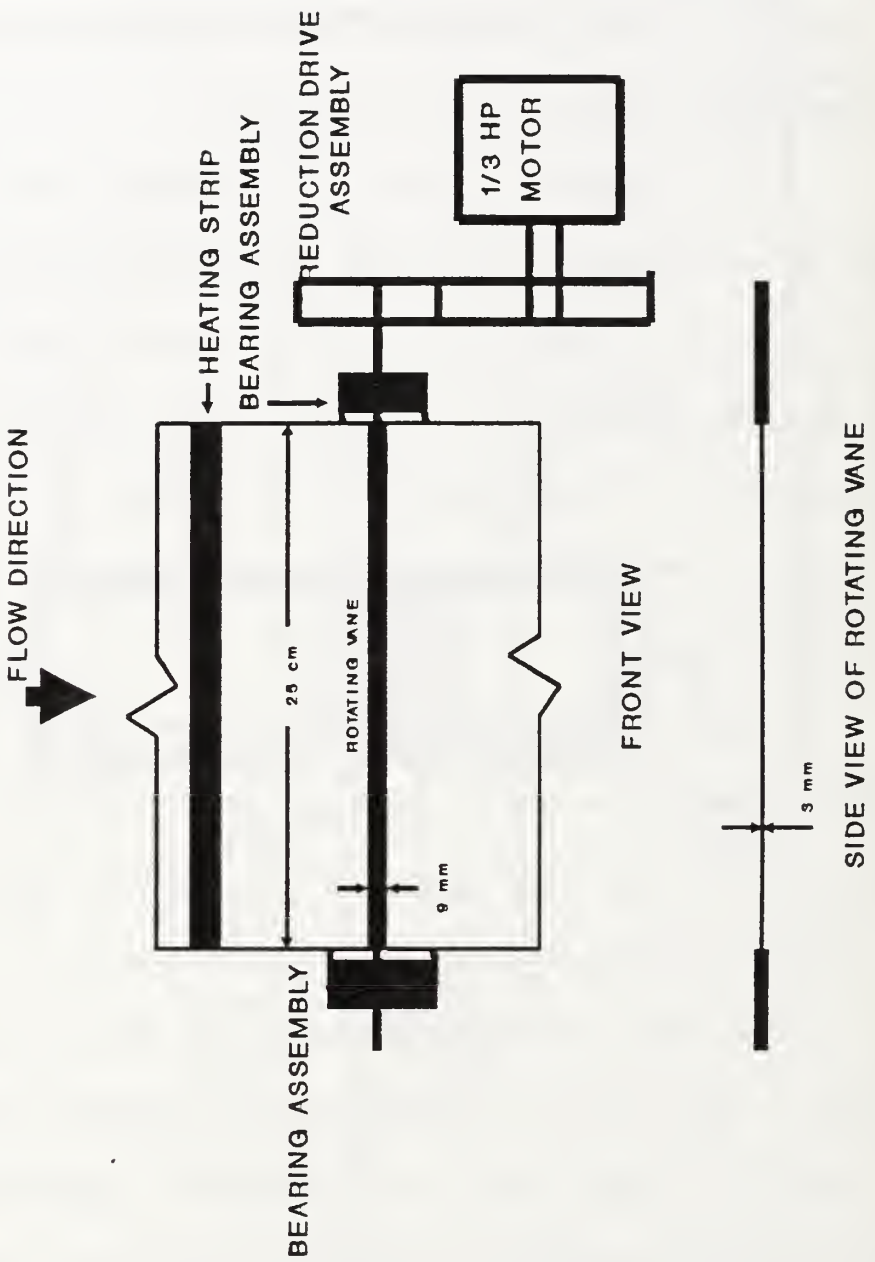

Figure 2. Rotating vane assembly.

grooves. These grooves housed the flush mounted heating strips. One such heating surface groove is shown in Figure 3. Finally, a vertical 0.120 cm deep groove was milled to house the electrical leads to the heating strips. A front view of the test surface is shown in Figure 4. A side view of the channel is shown in Figure 5.

Before mounting the heater strips to the board, 5 copper constantan thermocouples were mounted in the deepest groove for each heater with a resulting total of fifty thermocouples for the entire test surface. The thermocouples were equally spaced 3.1 cm apart. The two end thermocouples in each groove were made with 0.254 mm diameter wire and the three middle thermocouples in each groove were made from 0.127 mm diameter wire. Locations of the thermocouples are shown in Figure 4 for the top heater.

All of the thermocouples were mounted into the deepest grooves using a low thermal conductivity epoxy (Omega bond 100). This served to effectively reduce the conduction losses out the back of the board. A very thin layer of Omega 101 was placed in the area of the heating strips where thermocouples would be measuring. The heating strips were then carefully

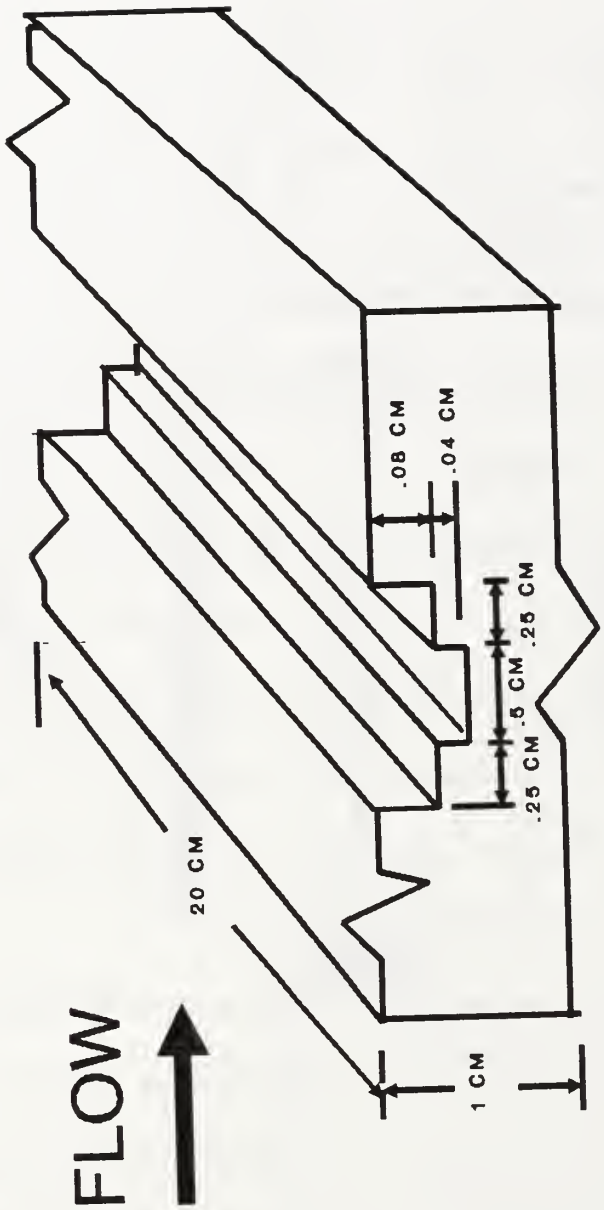

Figure 3. One heating surface groove.

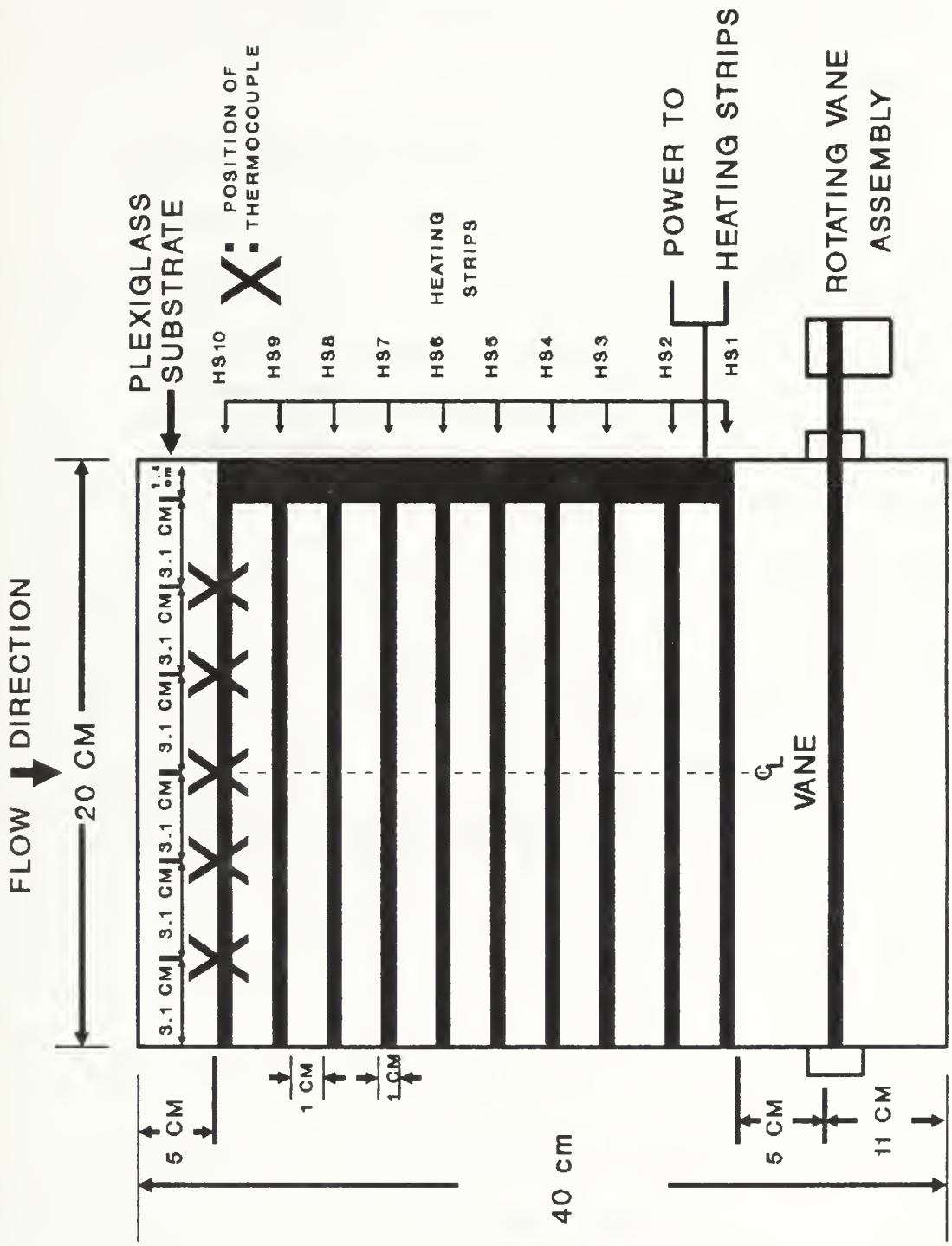

Figure 4. Front view of test surface.

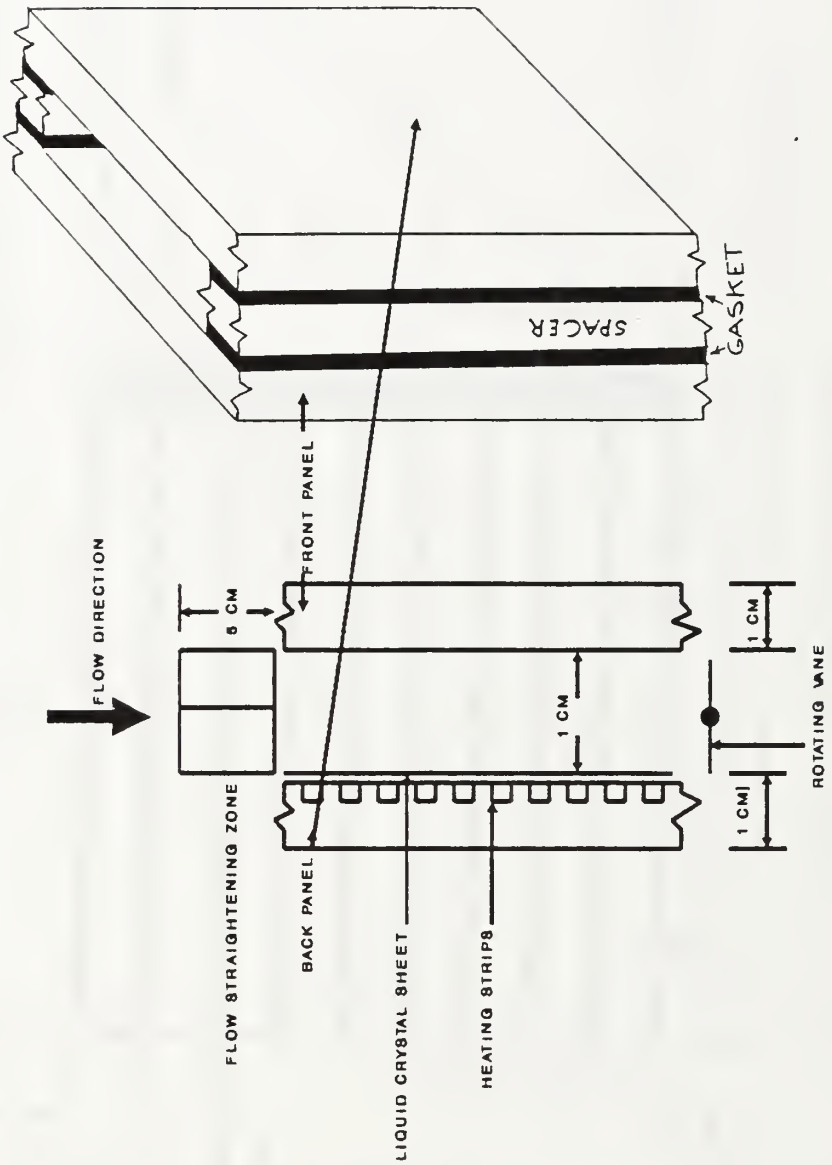

Figure 5. Side view of test surface.

mounted in their respective grooves using a very thin coat of Omega bond 100 to ensure a flush mounted heating surface.

2. Power Distribution System

A schematic of the power distribution panel is shown in Figure 6. Power to the individual heaters was supplied by a 0-10 A, 0-5 V DC power supply. This supply was connected to a common bus which provided power to each of the ten individual heating strips. Each heater was connected in series with a precision resistor (R=2.01±0.005$Ohms$). The data acquisition system obtains voltage readings across the entire bus bar(V_{Tot}) and across each heater(V_{Heat}). From these two measured values, the input power to each heater was easily computed using the following relation:

$$Power = \left(\frac{V_{Tot} - V_{Heat}}{R}\right) * V_{Heat}$$

3. Data Acquisition Assembly

The Data Acquisition assembly consisted of a HP 9000 computer system and a HP 3852 Data Acquisition Unit. The computer instructed the data acquisition system to monitor temperatures from desired thermocouples and measure the power

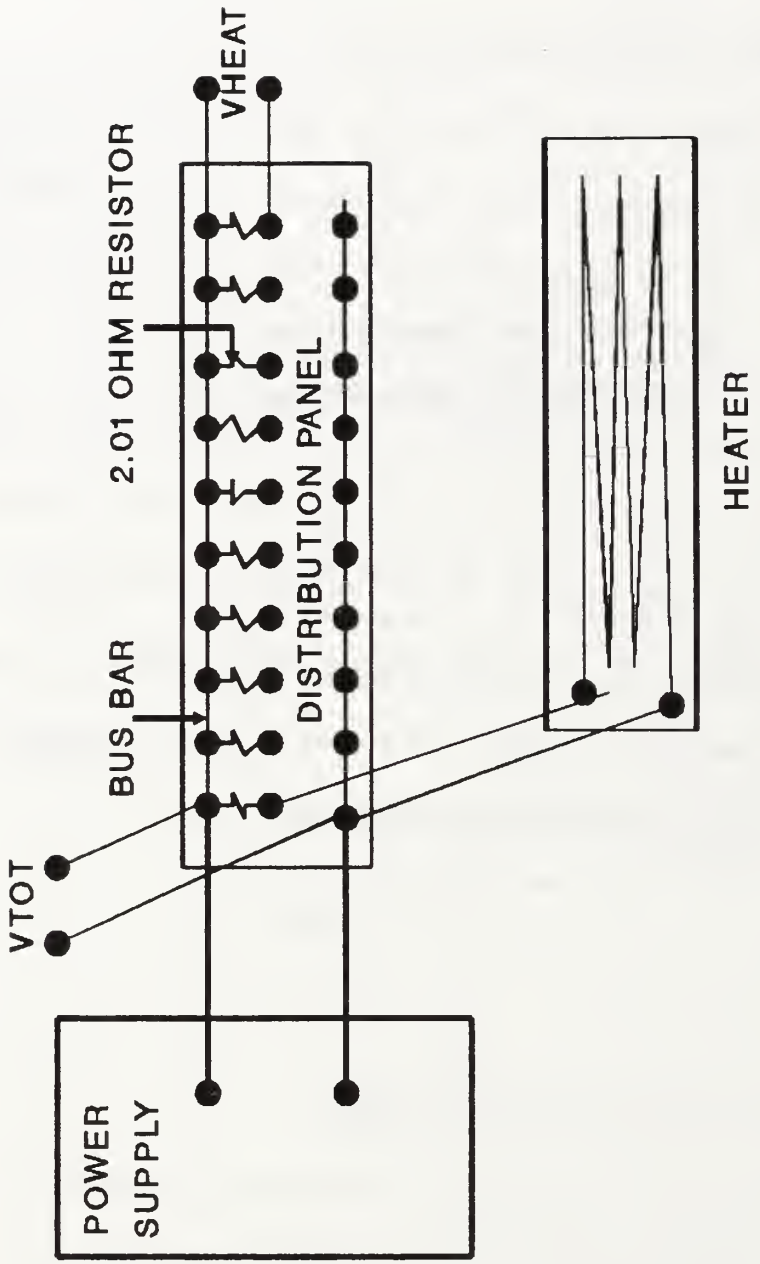

Figure 6. Power Distribution system.

delivered to each heating strip. Only selected thermocouples were scanned for each data run, depending upon the information desired. The scan rate was 5 samples/second for each thermocouple.

B. LIQUID CRYSTALS

The surface temperature patterns were visualized using 0.762 mm thick, 20 cm by 20 cm in area, Hallcrest thermochromic liquid crystal (TLC) sheets. The crystals in these sheets display shades of green and blue in reaction to temperature changes in the approximate range of 30 to 35 $^{\circ}C$.

To use the liquid crystals for this particular experiment, it was necessary to cut the TLC sheet to fit precisely over the entire test surface, ensuring that it was perfectly smooth in order not to disturb the flow. Once the liquid crystal was over the heaters, the temperature distribution on the surface could be easily visualized.

C. EXPERIMENTAL PROCEDURE

The pulsatile flow study investigated four different heat fluxes, five different Reynolds numbers and four different vane rotation frequencies. All data runs were conducted with

all heaters powered. At first all thermocouples were scanned to determine if there were any obvious regions of interest since this was the first time this experiment had been run. It was then determined to take continuous readings on the center thermocouple on the top heating strip on the test surface (HS10). The scanning rate was about 5 samples/second. Data was taken continuously for 5 minutes on that single thermocouple after a nominal steady state condition had been reached for each heat flux, flow rate, and vane frequency.

During each run, thermocouples were scanned on the remaining heating strips to determine if there were any noticeable effects of flow pulsations. In addition, adjacent thermocouples on each side of the center were scanned to determine spanwise effects. At low Reynolds numbers and high heat fluxes, opposed mixed convection effects were pronounced. For these conditions large timewise fluctuations in surface temperatures were found. This led to the second series of experiments and the investigation of mixed convection effects in the vertical channel. While conducting these runs, no vane rotation was employed.

Several data runs were conducted in order to investigate the opposed mixed convection effects. Four different heat fluxes (505,1050,1600,2702 W/m^2) and five different Reynolds numbers (500,1000,2000,4000,7300) were utilized. The center thermocouples on the five alternate heaters (HS10,8,6,4,2) were scanned in order to ascertain the local transient temperature variation over a five minute span along the entire test surface. In addition, adjacent thermocouples to the center thermocouple were also analyzed on the top heater (HS10), middle heater (HS5), and bottom heater (HS1) in order to ascertain spanwise variation in surface temperature. In addition, temperatures were measured after powering every alternate heater. Finally, center temperatures on selected heaters were also measured in order to determine transient response to sudden powering of the heating strips. The fluid temperature at the channel inlet was measured at two locations; in the inlet sump and the inlet to the test section. These two values were always within $0.1^{\circ}C$.

III. RESULTS

A. DATA ANALYSIS

A simple energy balance was performed around each heater. From the following relation, neglecting conduction losses, the rate of energy removed by convective heat transfer is:

$$Q_{Conv}=Q_{Heat}$$

Where Q_{Heat} is the power supplied to each heater in watts.

Once the value of Q_{Conv} is known, the heat flux, q'', to each heater can be determined by the following relation:

$$q''=\frac{Q_{Conv}}{A_s}$$

Where A_s is the surface area of the heater.

The next step was to calculate the average heat transfer coefficient **h**. Newton's law of cooling was utilized relating **h** with the above heat flux and the temperature difference, ΔT. ΔT was the temperature difference between the heater surface temperature and the average inlet fluid

temperature. The value of **h** was given by the following relation:

$$h=\frac{q''}{\Delta T}$$

The parameters describing the heat transfer for a given vane rotation frequency are: the flux based Grashof number (Gr^*), the average Nusselt number (Nu), and the Reynold's number (Re). The length scale used to calculate Nu and Gr^* was the heater width. The characteristic length used in the calculation of the channel Reynold's number was as follows:

$$L_c=\frac{A_c}{P}$$

Where A_c is the cross-sectional area of the channel, and P its perimeter.

The flux based Grashof number was calculated based on the following expression:

$$Gr^*=\frac{g\beta q''L^4}{k_f\nu^2}$$

Where k_f ,g, β ,and ν were found in Reference 8. The local film temperature was defined by:

$$T_{Film}=\frac{T_{Heater}+T_{Inlet}}{2}$$

The average Nusselt number was calculated using the following expression:

$$Nu=\frac{hL}{k_f}$$

The Reynolds number was calculated by:

$$Re=\frac{VL_c}{\nu}=\frac{\dot{m}}{P\mu}$$

Where V is the average velocity of the fluid in the channel.

In order to clearly present the data on vane rotation at several downstream locations, a non dimensional length term was calculated as X/L, where X is the distance from the top edge of the test surface to the top edge of the heater in question and L is the overall length of the test section (20 cm).

The collected data were expressed as plots of:

- Avg Nu vs X/L for vane rotation data

The mixed convection portion of this study resulted in the following plots:

- ΔT vs time
- Avg Nu vs Re

B. PULSATILE FLOW RESULTS

The presentation and analysis of data in this section involved determining overall heat transfer characteristics for different vane rotation frequencies. Four different heat fluxes and five different Reynolds numbers along with four different vane rotation frequencies were utilized. All figures displaying pulsatile flow results show Nu variation for different heater locations (Nu versus X/L).

Figures 7-10 (q''=505W/m^2) show no clear trend of vane rotation either enhancing or deteriorating overall heat transfer. In every case the top heater, HS10 (X/L=0.95), always has the highest Nusselt number. This is expected since this is the first heater the flow encounters and therefore it is the coolest. The bottom heater, HS1 (X/L=0.95), is always one of the hottest heaters, regardless of vane rotation

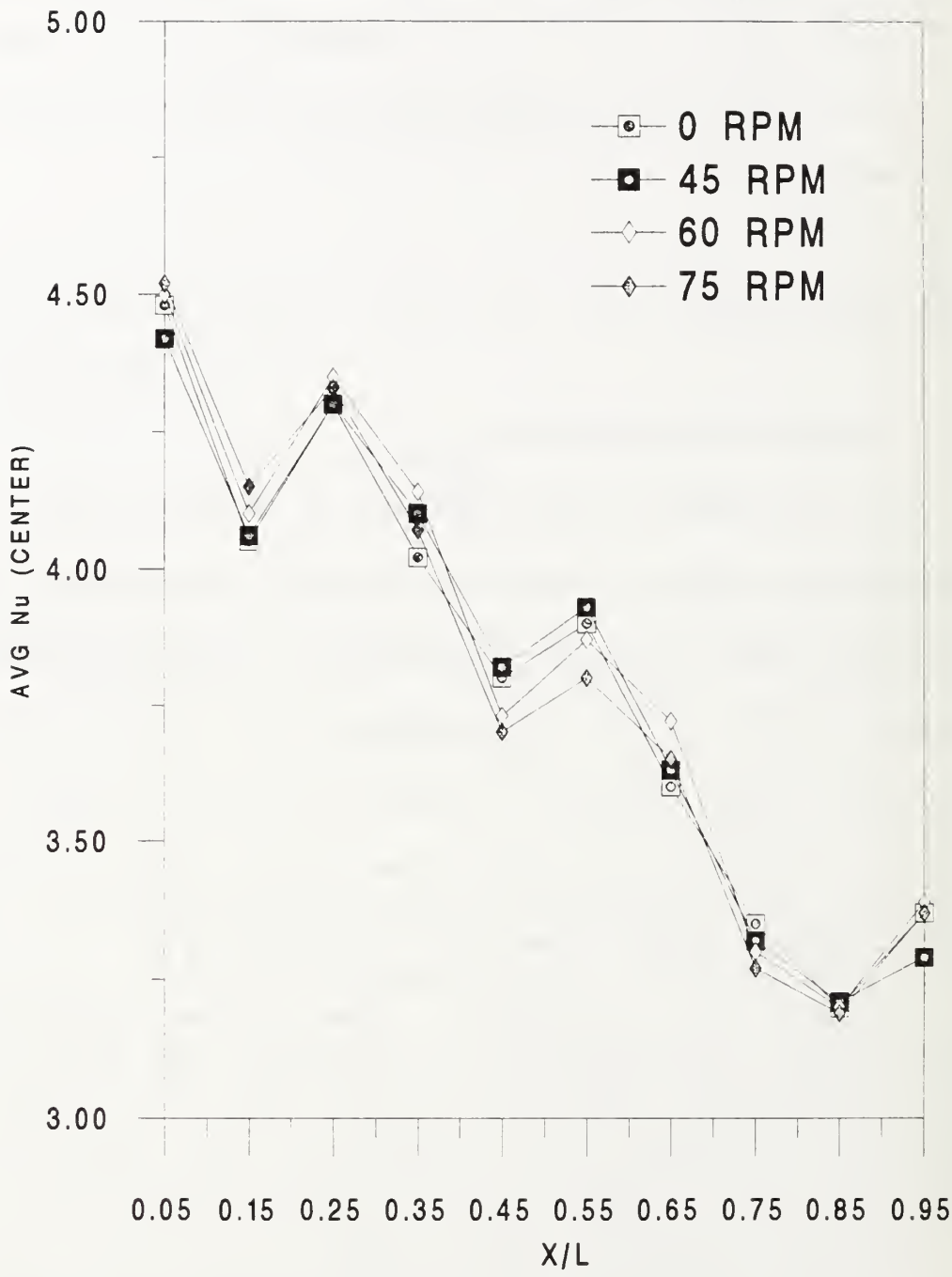

Figure 7. Average Nusselt number versus X/L. Heat flux =505 W/m^2 ; Re=2000.

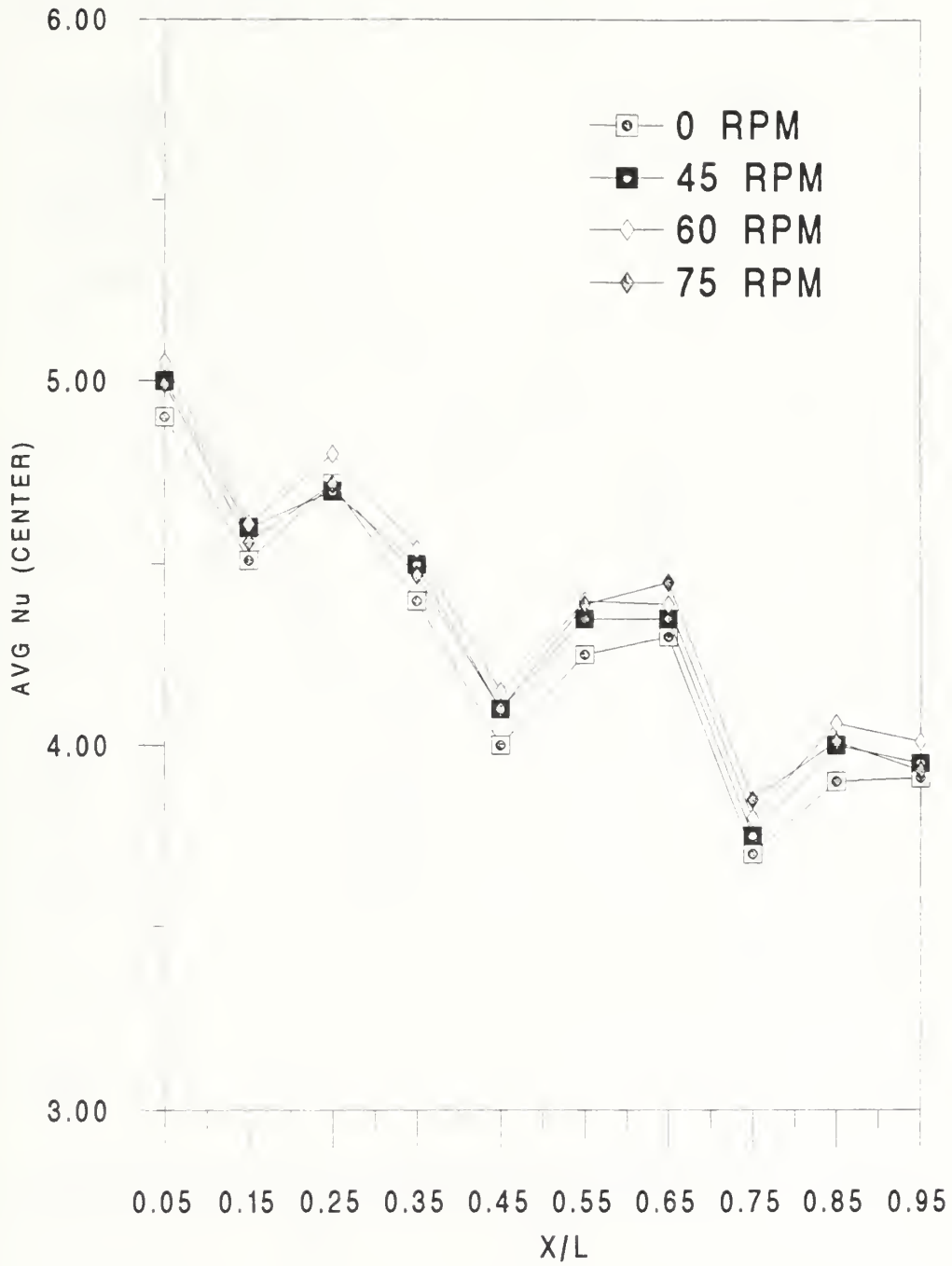

Figure 8. Average Nusselt number versus X/L. Heat flux=505 W/m^2 ; Re=3000.

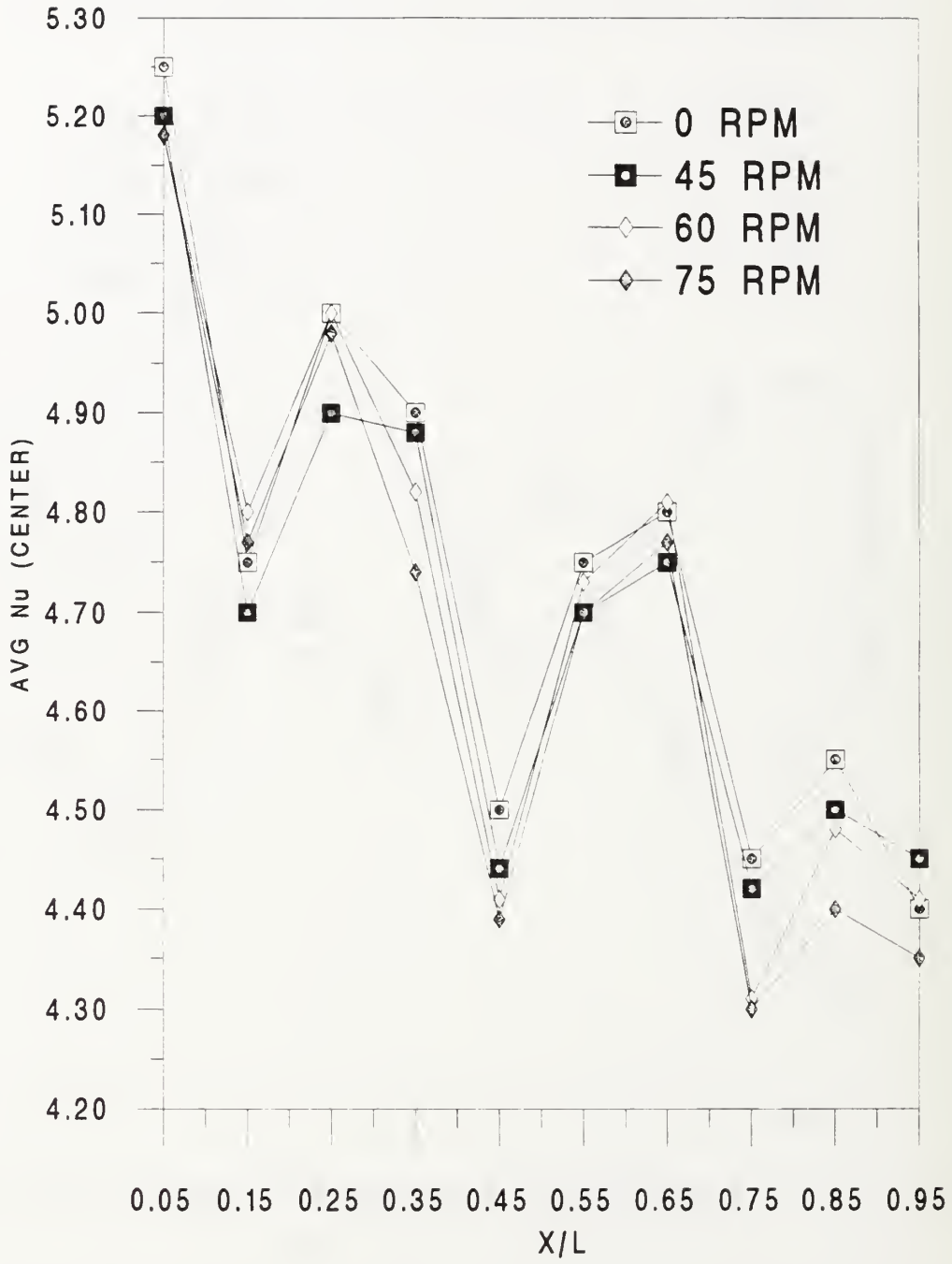

Figure 9. Average Nusselt number versus X/L. Heat flux=505 W/m^2 ; Re=5000.

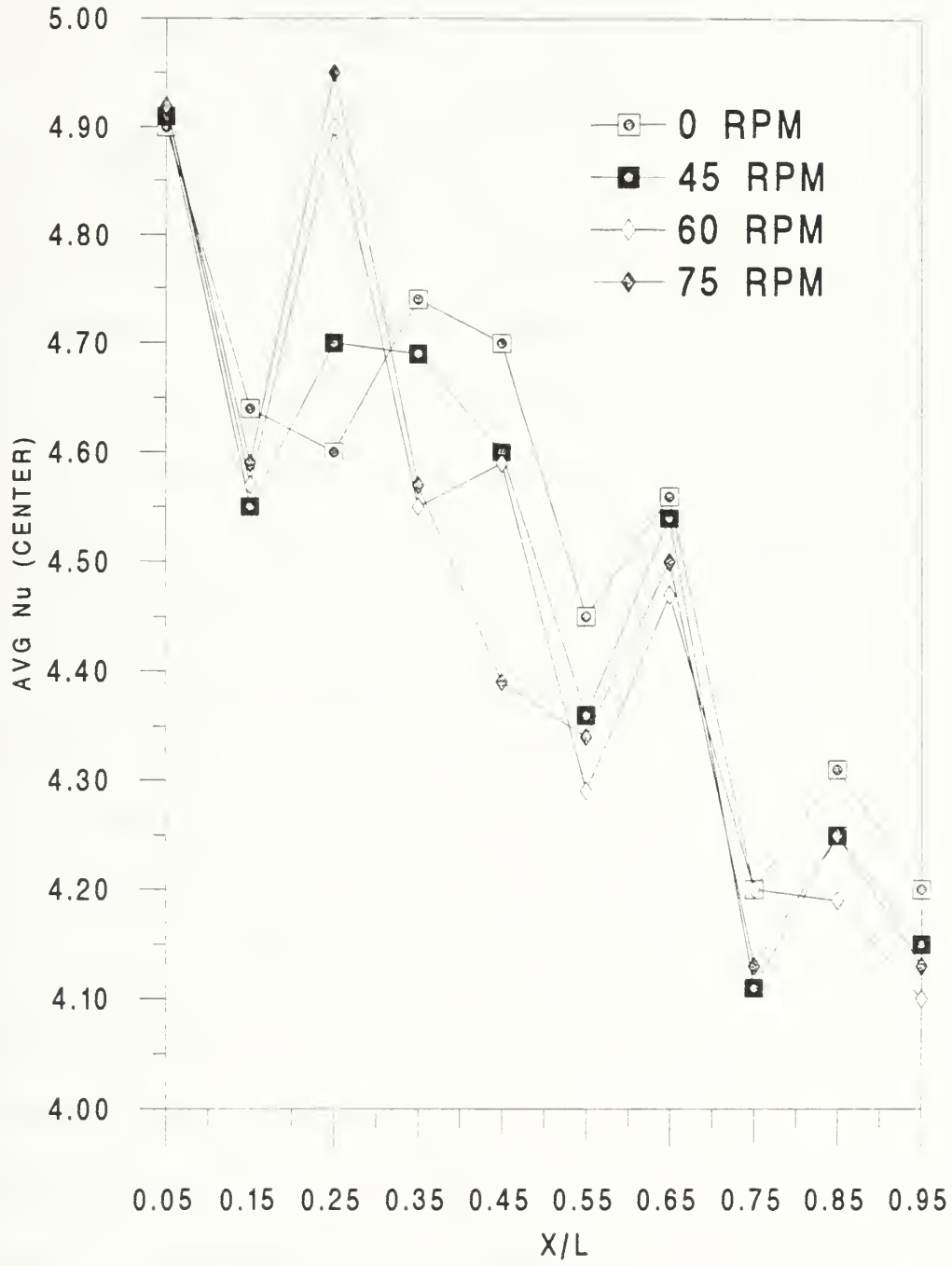

Figure 10. Average Nusselt number versus X/L. Heat flux=505 W/m^2 ; Re=8000

frequency. In Figure 10 (Re=8000), it is seen that the Nu values for all heaters are about 5% less than the corresponding values in Figure 9 (Re=5000).

The heat flux was then increased to 1050 W/m^2 and the results are shown in Figures 11-14 for four values of Re. As shown in Figure 11, opposed mixed convection effects are important for Re=1000 since the bottom heater, HS1 (X/L=0.95), is the coolest. The flow appears to have regions of reversal due to buoyancy. As the Reynolds number was increased to 2000, the results shown in Figure 12 are similar to Figures 7-10, displaying predominate forced convection effects. It is worth noting that in Figures 11 and 14, vane rotation is actually hurting heat transfer. The 0 RPM curve is always demonstrating higher Nusselt numbers than the other vane rotation curves. Figure 15 shows results for q''=1600W/m^2 and Re=2000. This figure is representative of all the data runs for this heat flux. It is difficult to say, outside the uncertainty for Nu as seen in Appendix A, whether rotation is either enhancing or deteriorating heat transfer. There is a wide disparity in the trend of average Nusselt based on heater location.

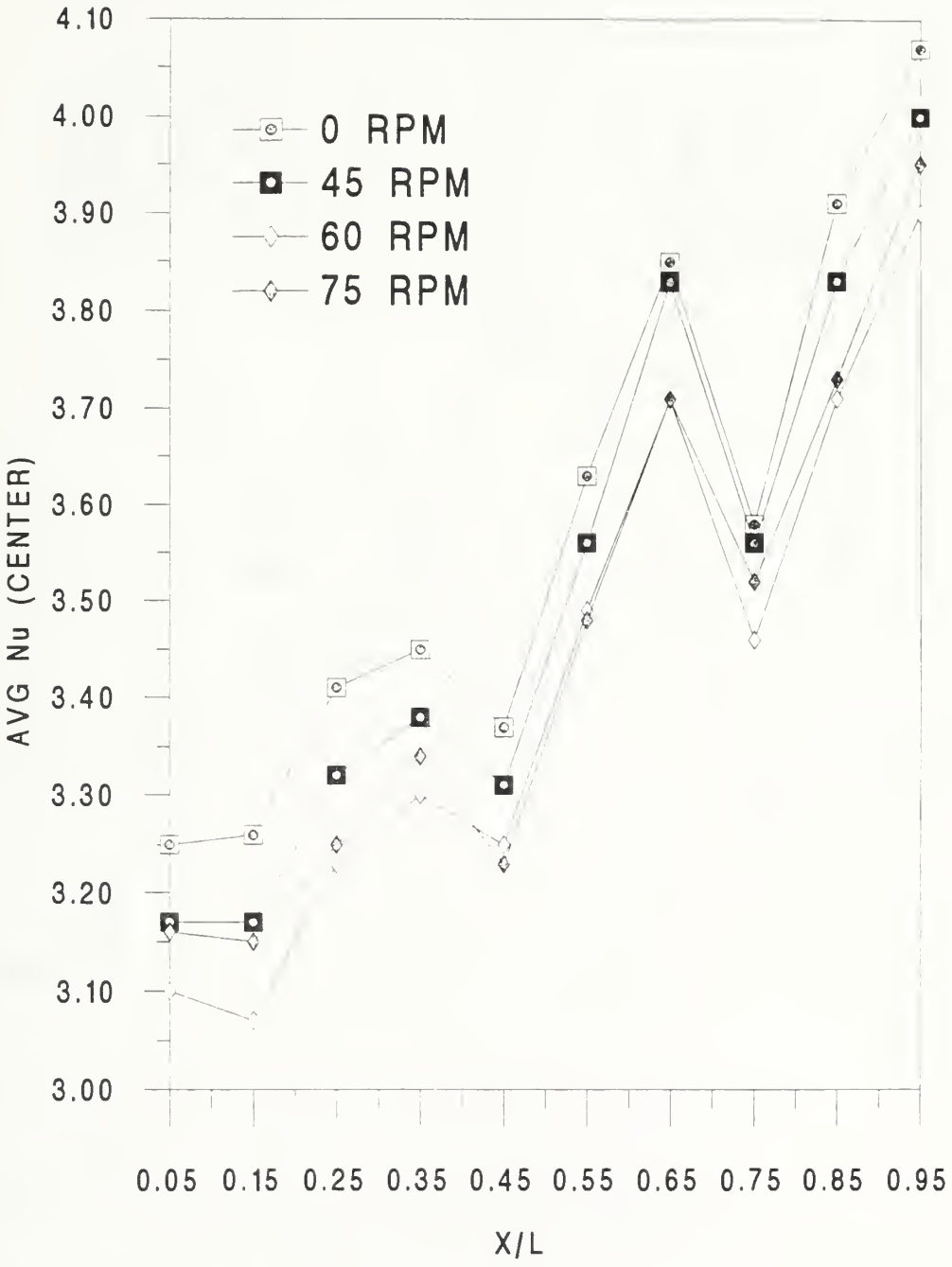

Figure 11. Average Nusselt number versus X/L. Heat flux= 1050 W/m^2 ; Re=1000.

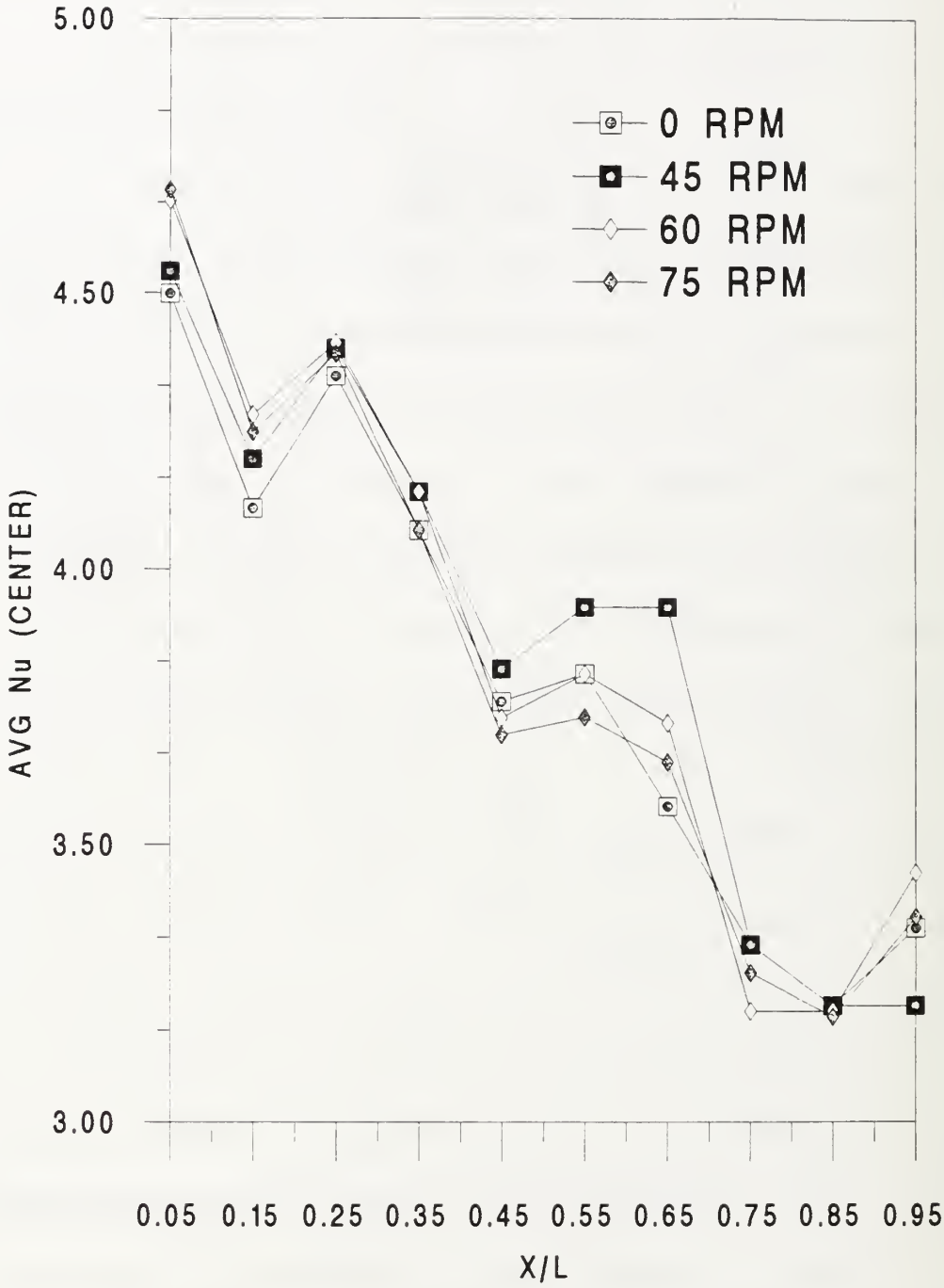

Figure 12. Average Nusselt number versus X/L. Heat flux= 1050 W/m^2 ; Re=2000.

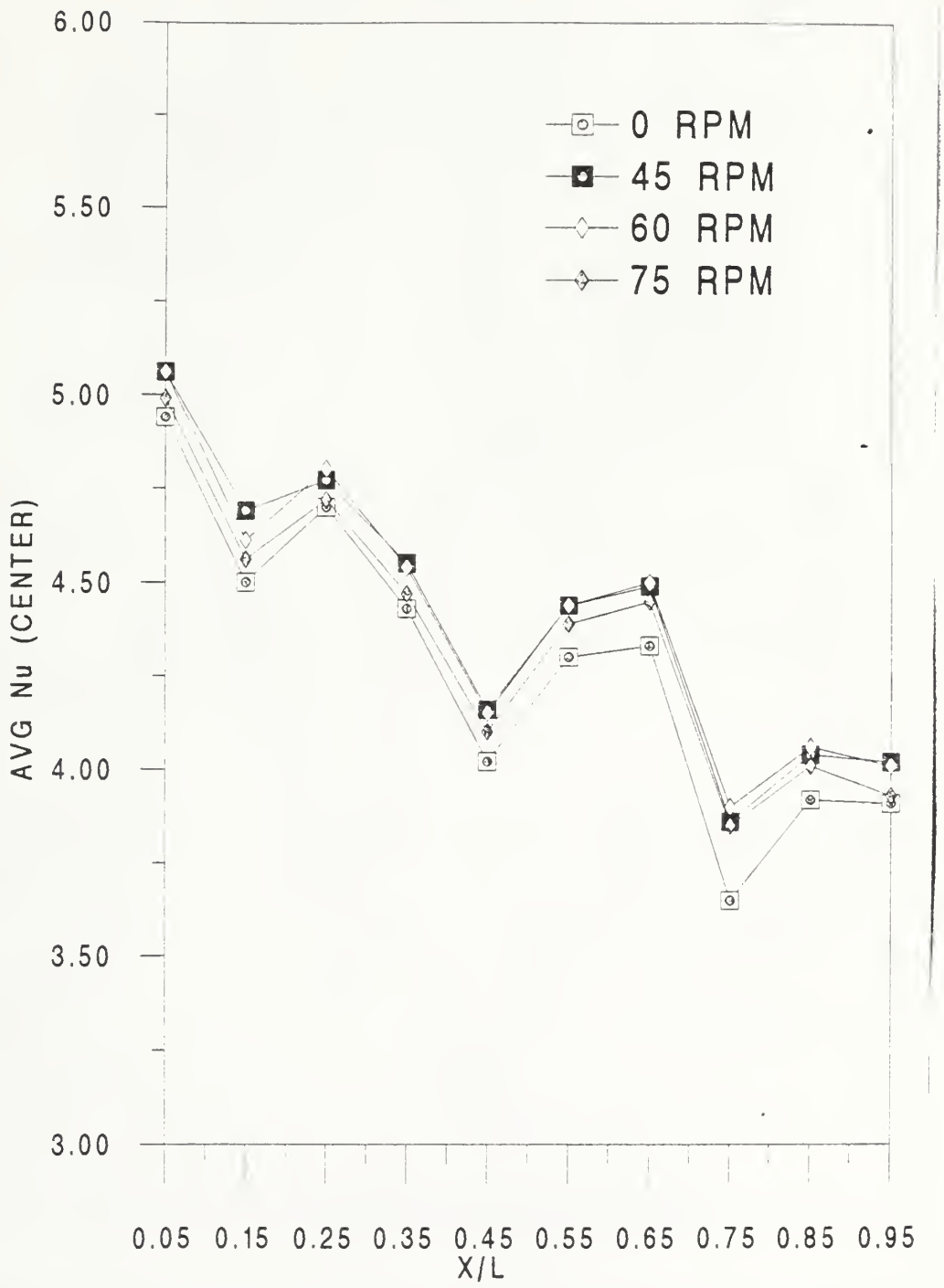

Figure 13. Average Nusselt number versus X/L. Heat flux= 1050 W/m^2 ; Re=3000.

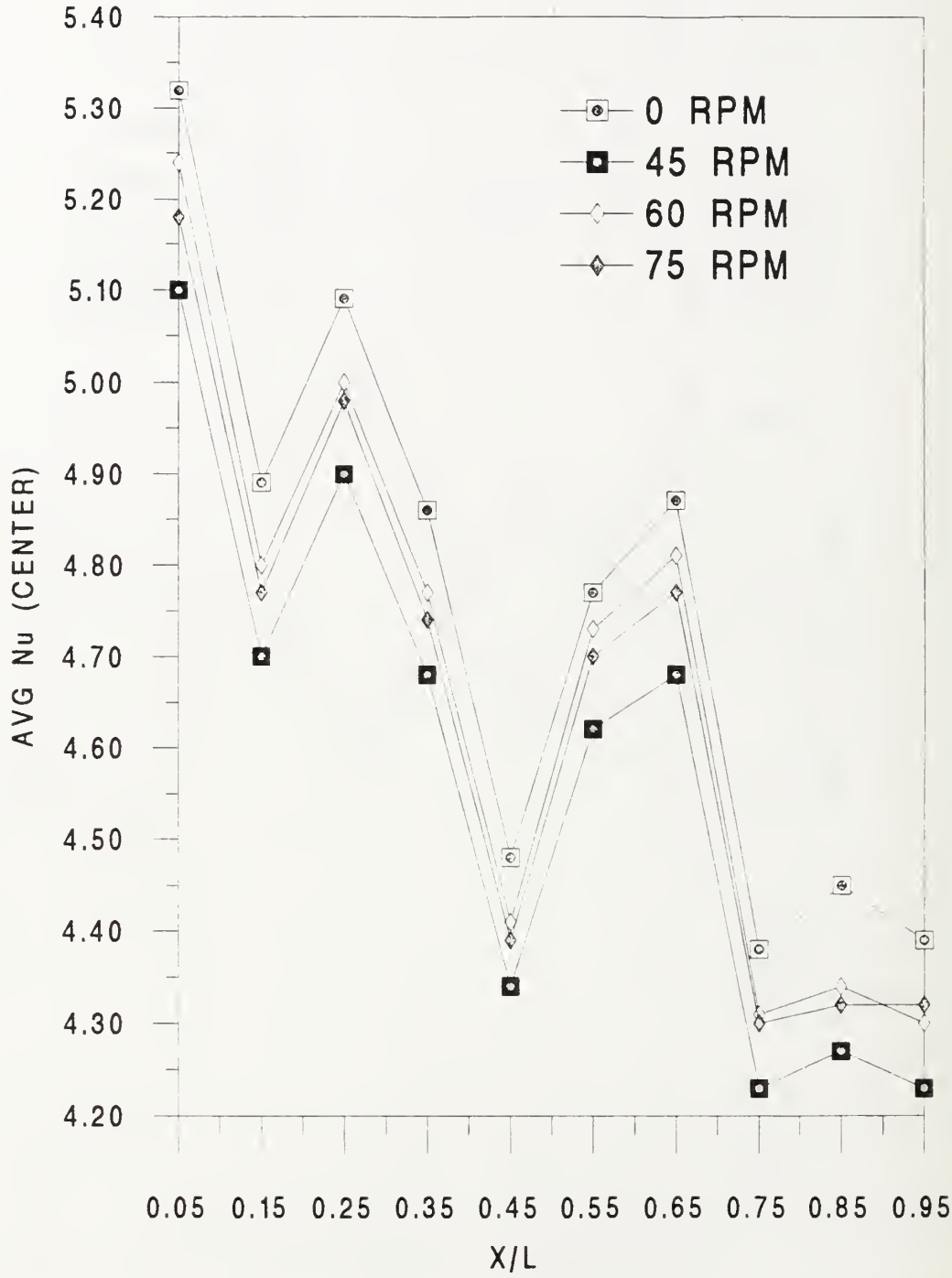

Figure 14. Average Nusselt number versus X/L. Heat flux= 1050 W/m^2 ; Re=5000.

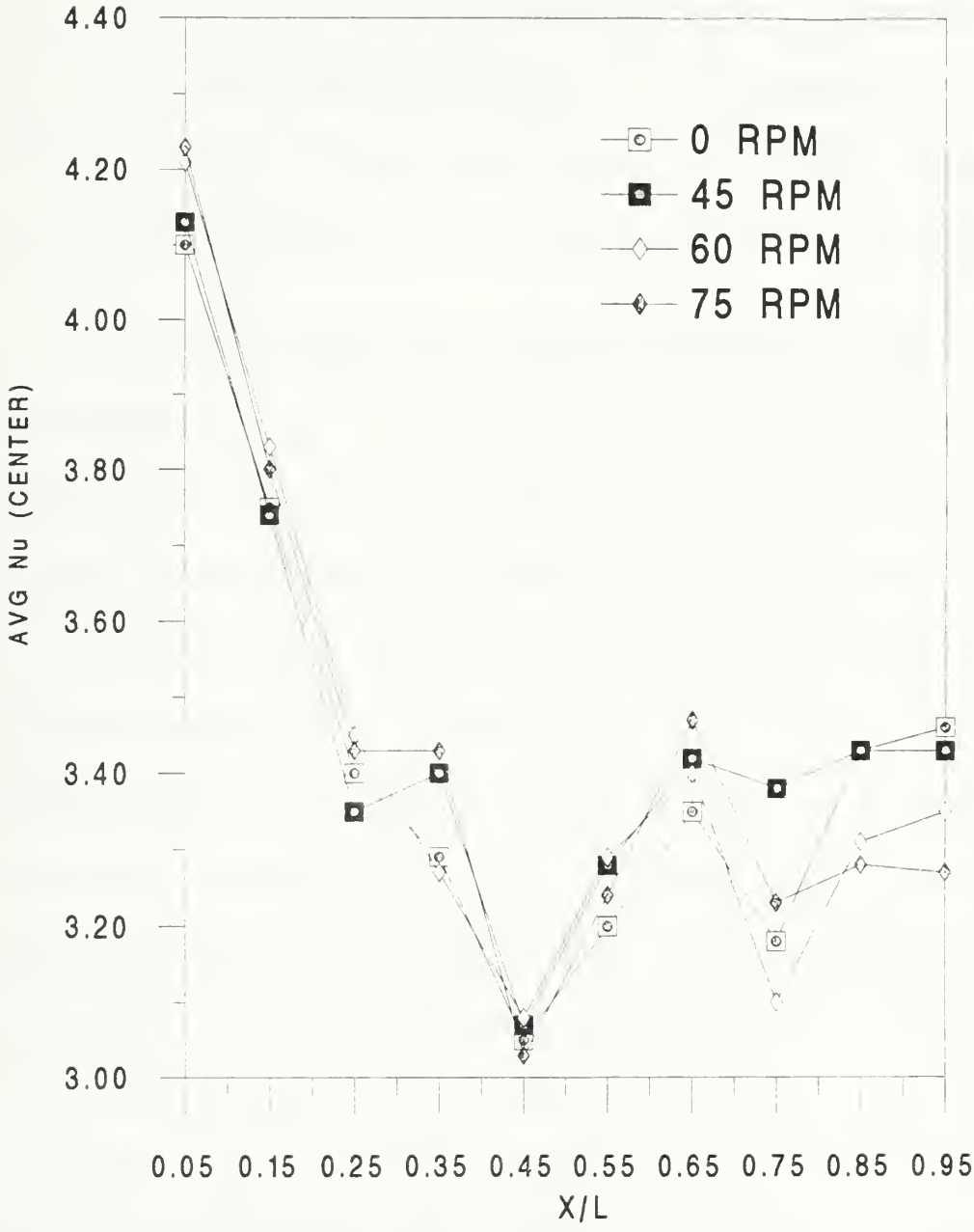

Figure 15. Average Nusselt number versus X/L. Heat flux= 1600 W/m^2 ; Re=2000.

Figure 16 shows results for $q''=2702W/M^2$ and Re=2000. Once again it is clear that there is no observable trend in average Nu outside the uncertainty range. As will be shown in the following section, this is probably due to the fact that mixed convection effects have become predominant and wide fluctuations in temperature are causing erratic Nu results.

C. MIXED CONVECTION RESULTS (NO VANE ROTATION)

In order to fully investigate the opposed mixed convection effects, four different types of data were taken. First, with all heaters powered, steady state temperatures were measured on the center thermocouple of five different heaters (HS10,8,6,4,2). Second, spanwise variation in temperature was measured on three different heaters (HS10,5,1) using the five thermocouples under each heater. Third, every alternate heater was powered and temperatures were measured by the center thermocouple on each powered heater (HS10,8,6,4,2). Finally, temperatures were monitored following a sudden powering of selected heating configurations. All heaters were suddenly powered and transient temperatures were measured by the center thermocouples on heaters 10,8,6,4,2. Every alternate heater was then powered and transient temperatures

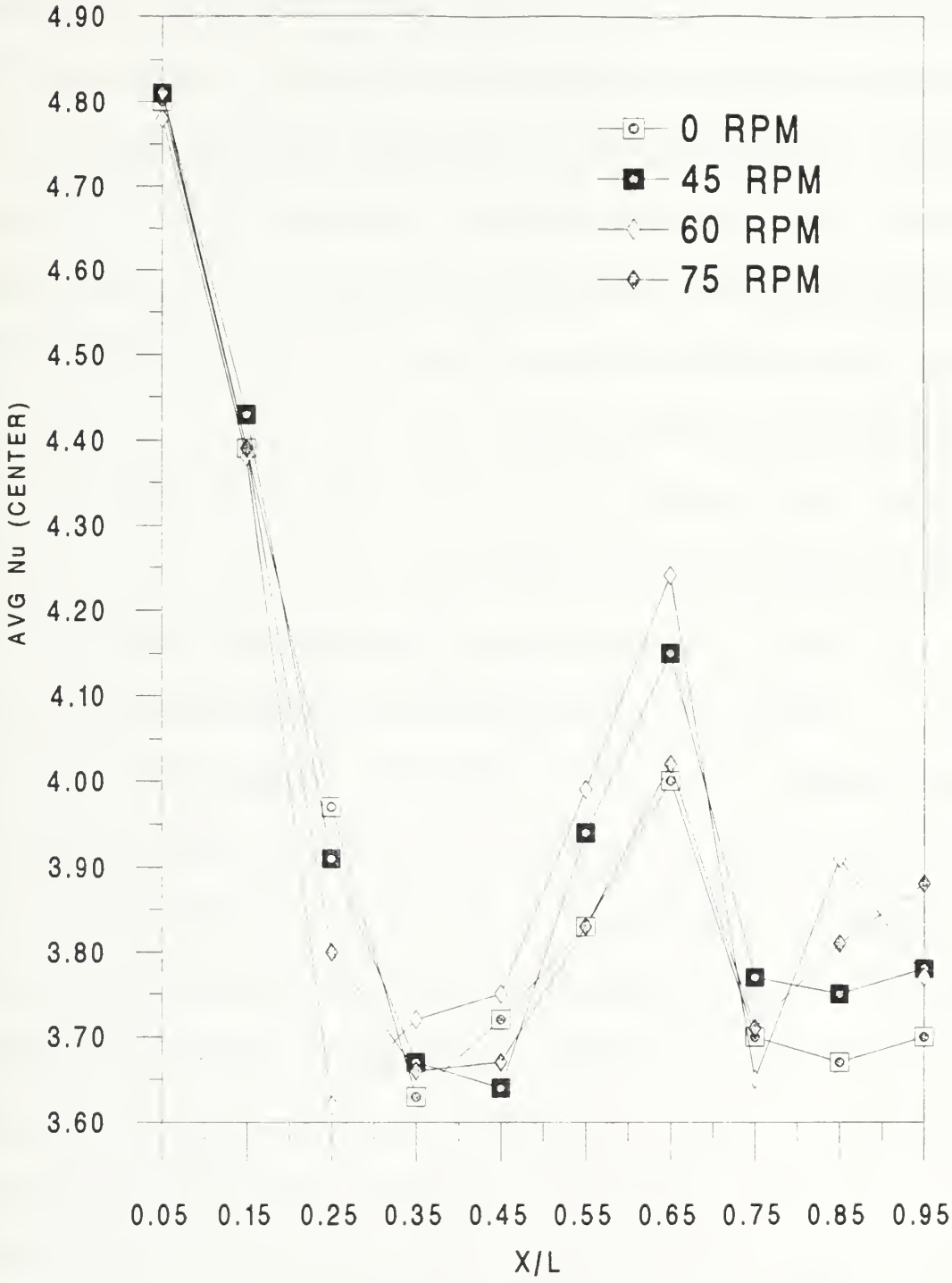

Figure 16. Average Nusselt number versus X/L. Heat flux= 2702 W/m^2 ; Re=2000.

were measured in the same manner. In addition, transient temperatures were measured by the center thermocouple of a heater not powered (HS9). The last set of measurements was made with only one heater powered (HS6). Transient temperatures were measured at the center of the powered heater and the center thermocouples of the adjacent unpowered heaters above (HS7) and below (HS5).

All results were plotted as Temperature Rise (K) versus Time (Seconds) and Nu versus Re.

1. Results under nominally steady conditions

Steady state temperatures were measured by the center thermocouple on five different heaters (HS10,8,6,4,2) for $q''=2510 W/m^2$. Figures 17-20 show results plotted as Temperature Rise versus Time. Figure 17 shows results for Re=1000. Large timewise fluctuations in the temperature are observed on all heaters. The largest temperature is seen on heater 10. This is expected because of the low Reynolds number and the resulting strong natural convection effects. At a higher Re of 2000, Figure 18, the fluctuations in temperature have become larger, with the top heater continuing to exhibit the largest temperature rise. Figure 19 shows the

results for Re=4000. At this Reynolds number, it is expected that forced convection will become dominant. The top heater now has the smallest temperature rise and the timewise fluctuations in temperature rise have become very small. However, large fluctuations in temperature are still seen on the other four heaters. Finally, the Reynolds number was increased to 7300 and the results are plotted in Figure 20. For this high Reynolds number it is seen that forced convection is clearly dominating and timewise fluctuations have disappeared on all heaters.

The heat flux was then reduced to $q''=1050 W/m^2$. In addition, the lowest Reynolds number for temperature measurements was reduced to 500 in order to further observe the buoyancy effects. Figure 21 shows results for Re=500. Heater 6 has now become the hottest heater and very little timewise fluctuation is observed. Heaters 2 and 4 are still exhibiting the smallest temperature rise as would be expected with dominating natural convection effects. The Reynolds number was then increased to 1000 and the results are shown in Figure 22. Heaters 2 and 4 continue to exhibit the lowest temperature rise; however, timewise fluctuations have

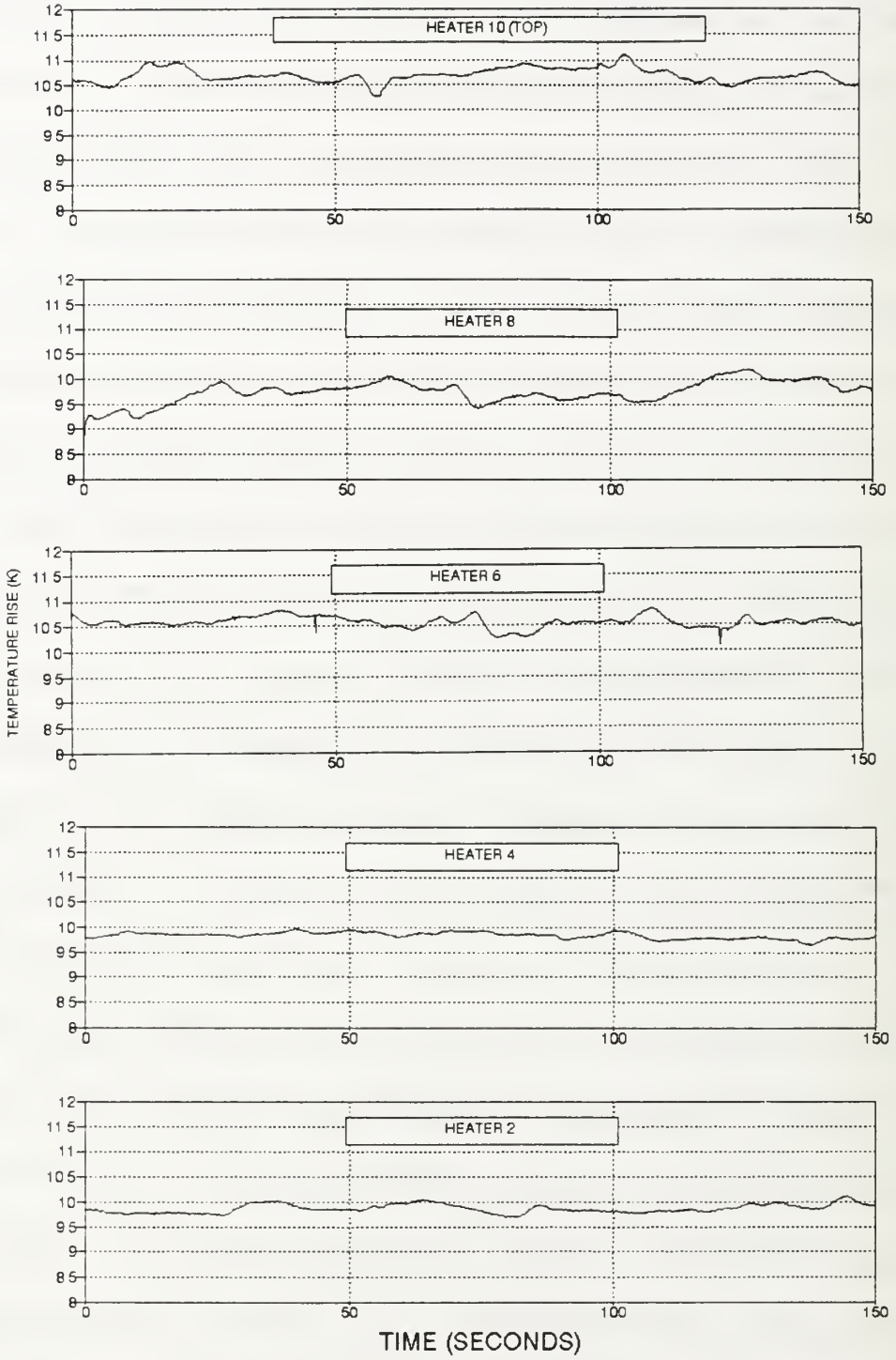

Figure 17. Temperature Rise versus Time. Heat flux= 2510W/m^2 ; Re=1000.

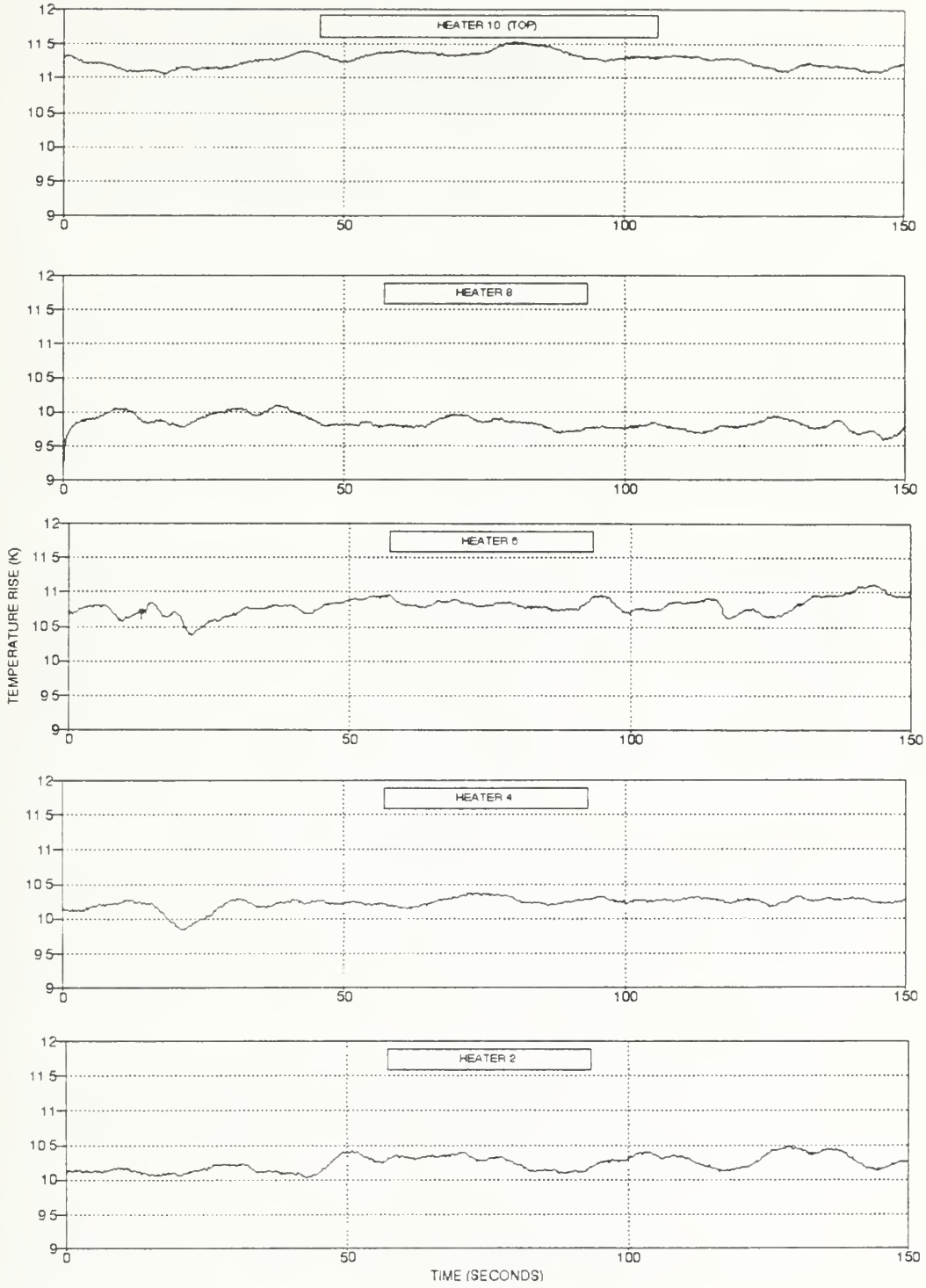

Figure 18. Temperature Rise versus Time. Heat flux= $2510 W/m^2$; Re=2000.

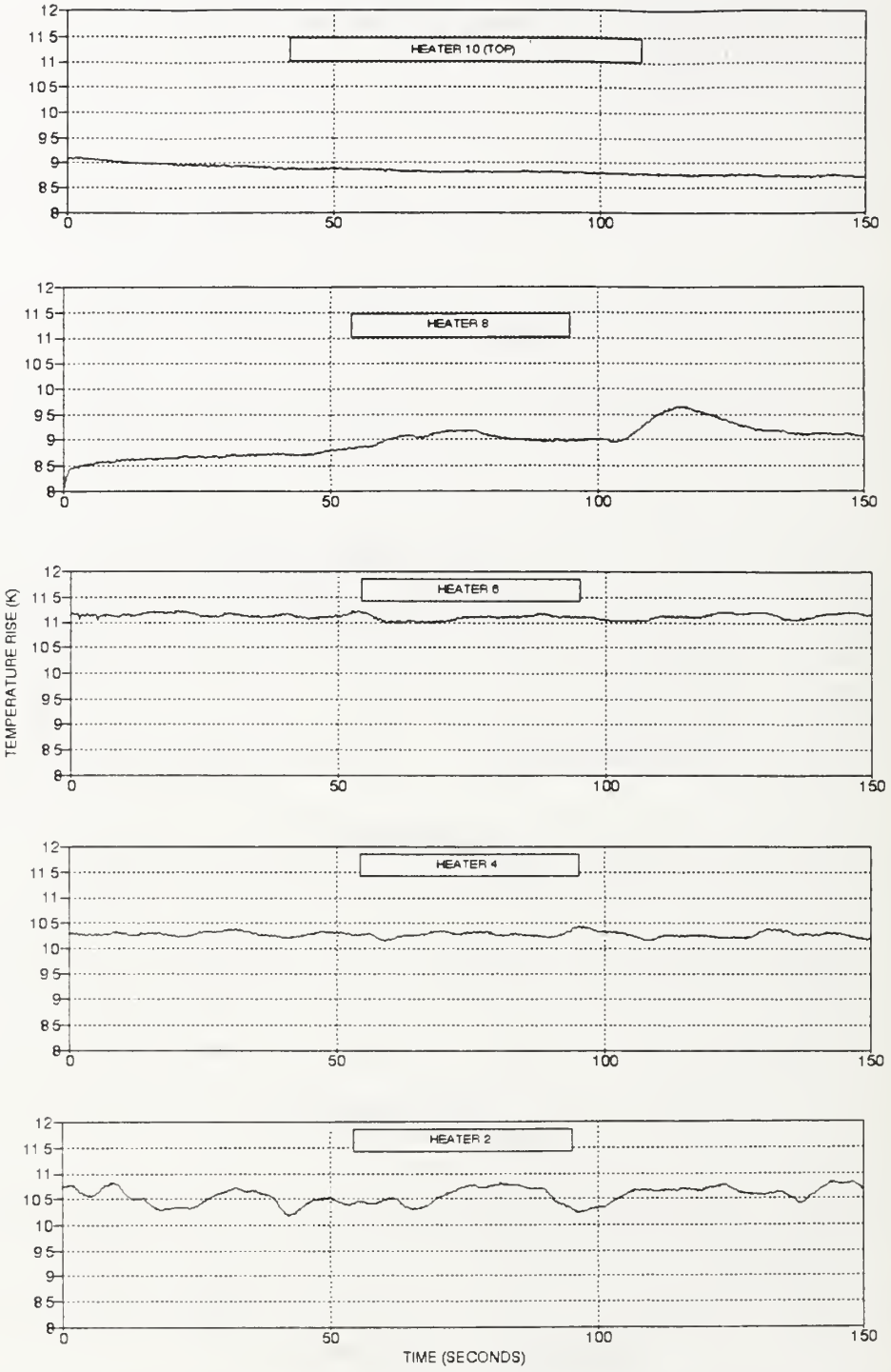

Figure 19. Temperature Rise versus Time. Heat flux= $2510 W/m^2$; Re=4000.

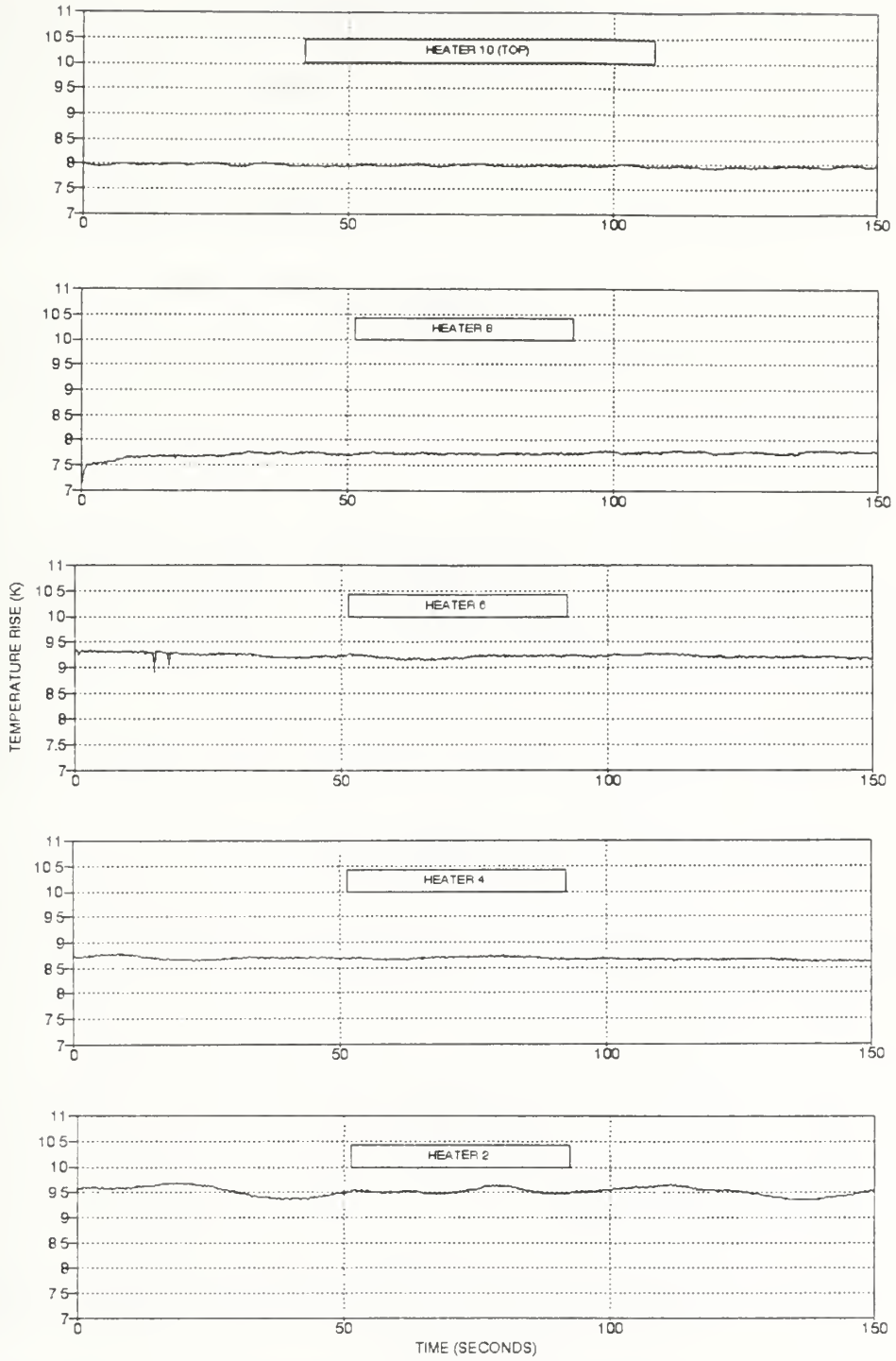

Figure 20. Temperature Rise versus Time. Heat flux= $2510 W/m^2$; Re=7300.

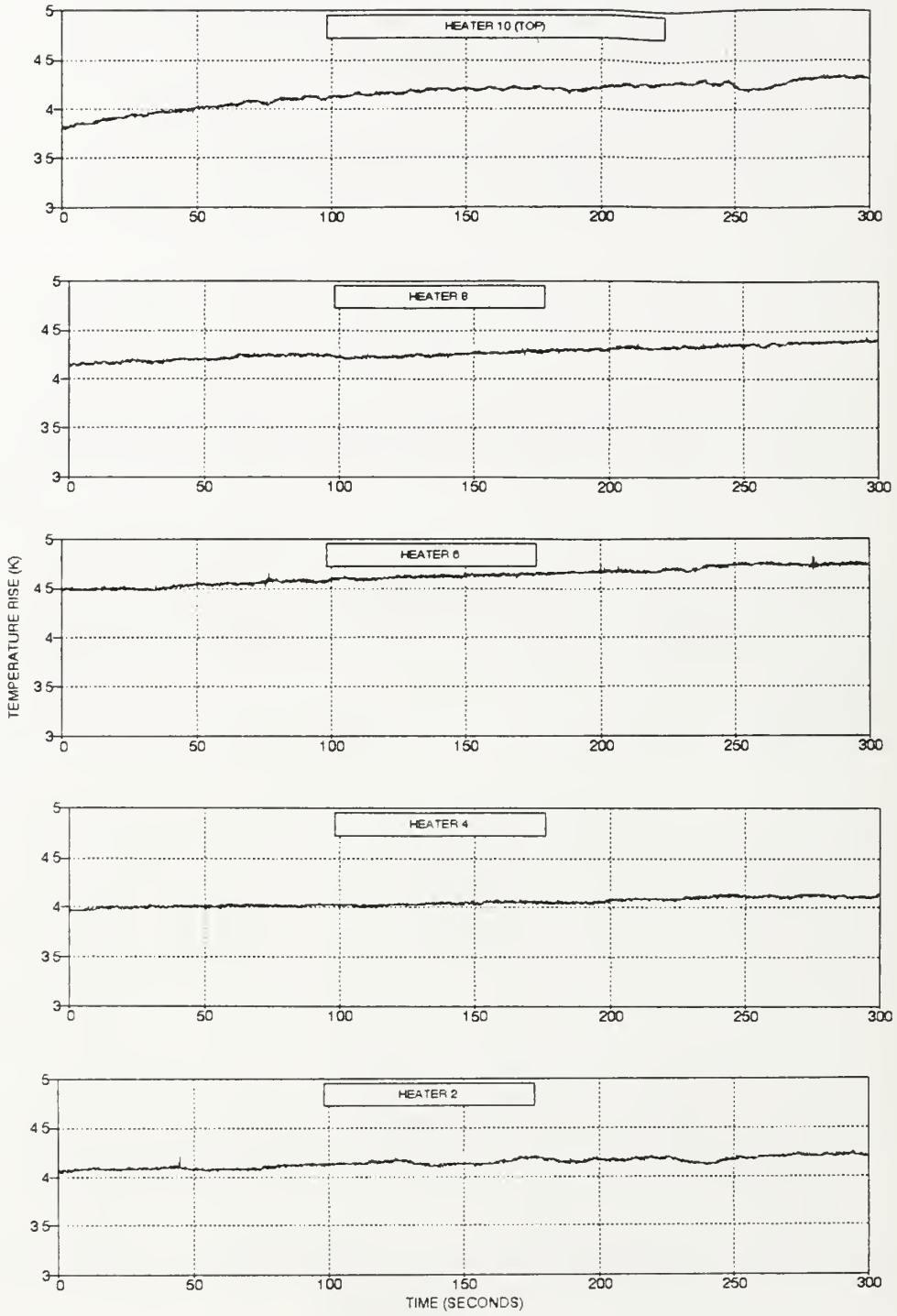

Figure 21. Temperature Rise versus Time. Heat flux= $1050 W/m^2$; Re=500.

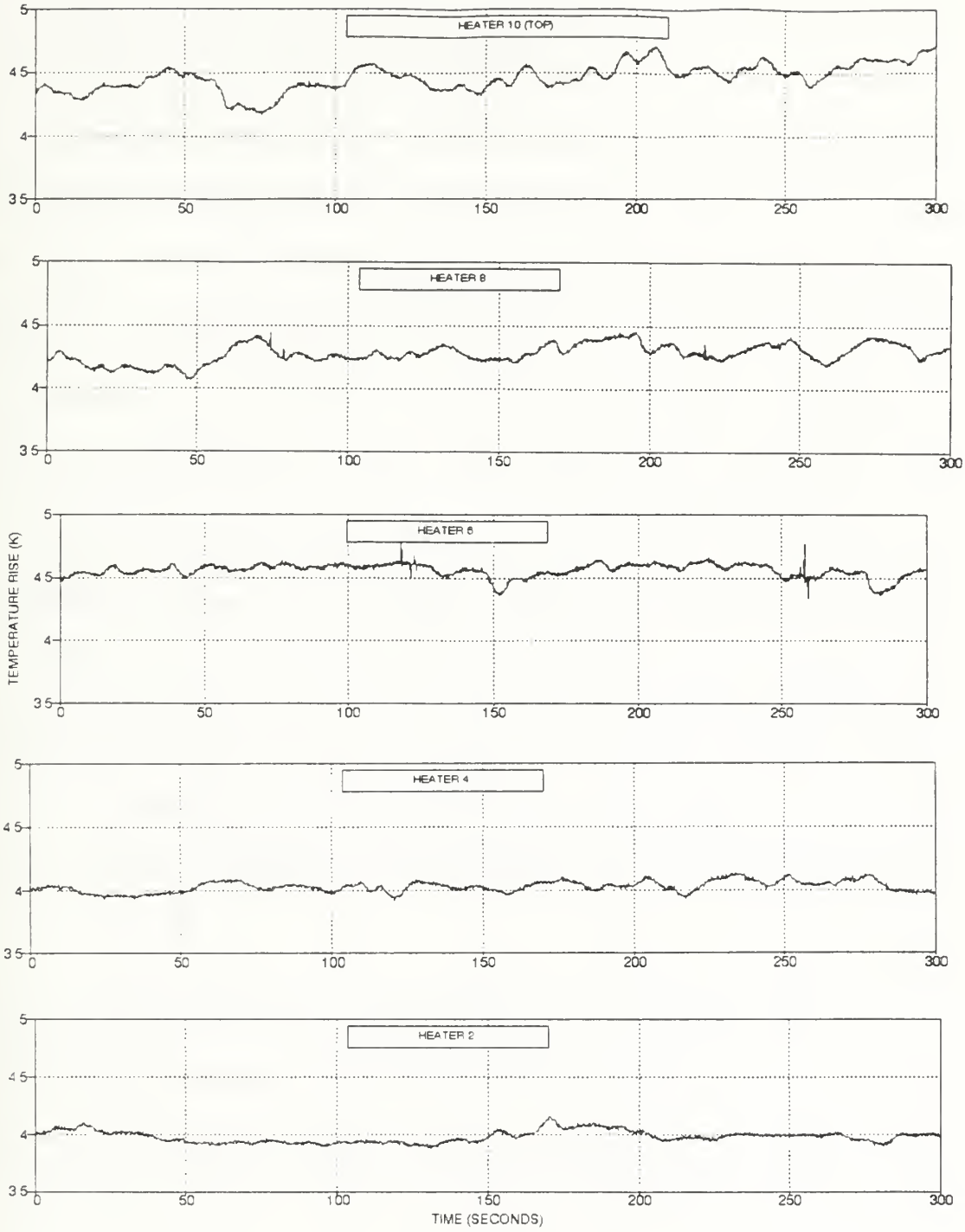

Figure 22. Temperature Rise versus Time. Heat flux= $1050 W/m^2$; Re=1000.

reappeared on all heaters. Figure 23 shows results for Re=2000. Heater 10 has the lowest temperature rise and is showing very little fluctuation in temperature. For the higher heat flux mentioned above, this smooth temperature curve was observed at Re=4000. Obviously, the lower heat flux has enabled the forced convection dominated regime to occur at a lower Re. The other heaters in Figure 23 further down in the channel are exhibiting very large fluctuation in temperature. The forced convection effect is still not dominant at these locations. Finally, the Reynolds number was increased to 4000 and the results are shown in Figure 24. The results show a forced convection behavior as the top heater is the coolest and the bottom heater the hottest, with no timewise variation in temperature observed on any of the heaters.

The next series of data was taken with every alternate heater powered (HS10,8,6,4,2) and the temperatures measured by the center thermocouple of those powered heaters. The heat flux was $q''=2505 W/m^2$.

The results for Re=500 are shown in Figure 25. As expected, heater 10 shows the largest temperature rise with

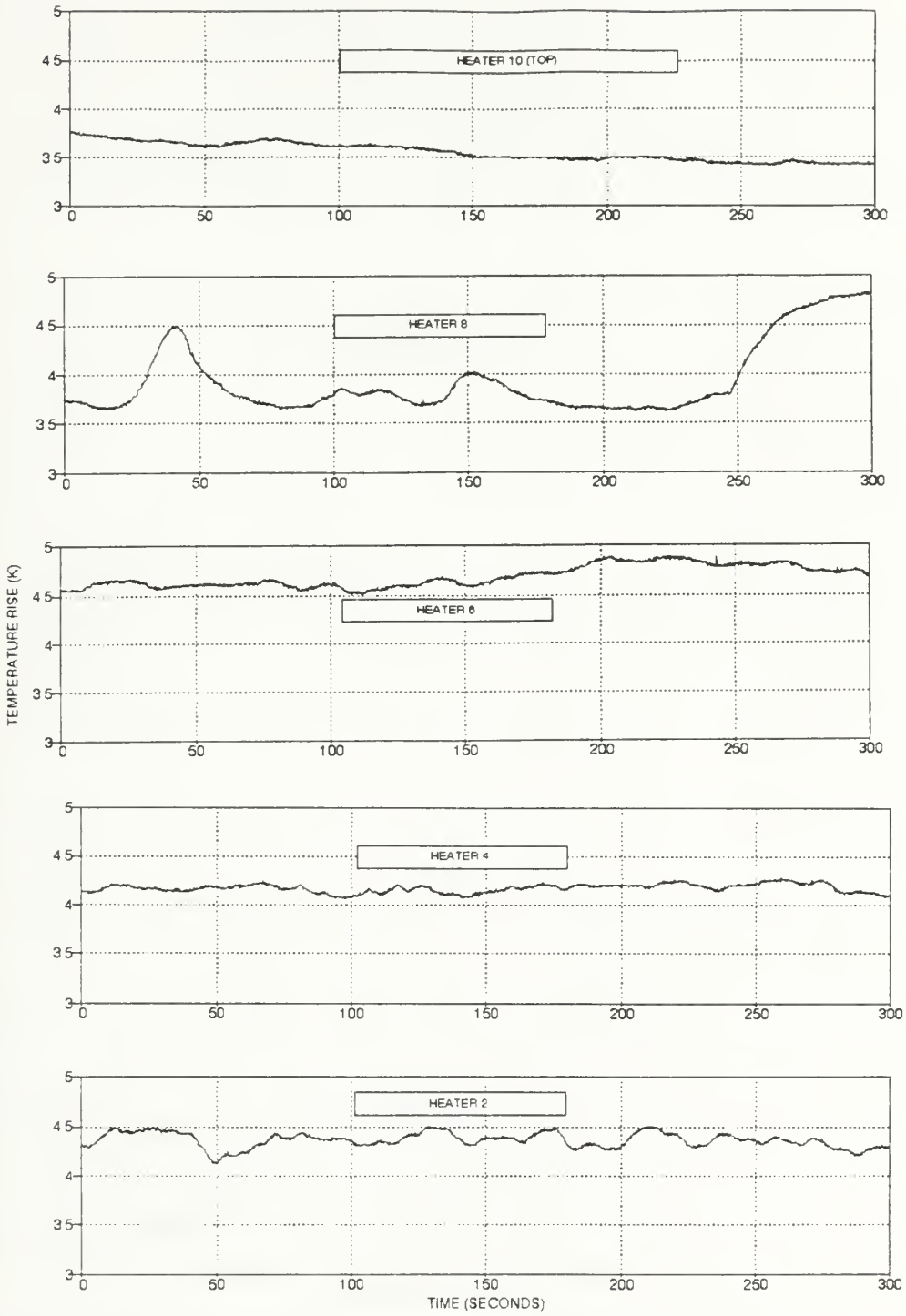

Figure 23. Temperature Rise versus Time. Heat flux= $1050 W/m^2$; Re=2000.

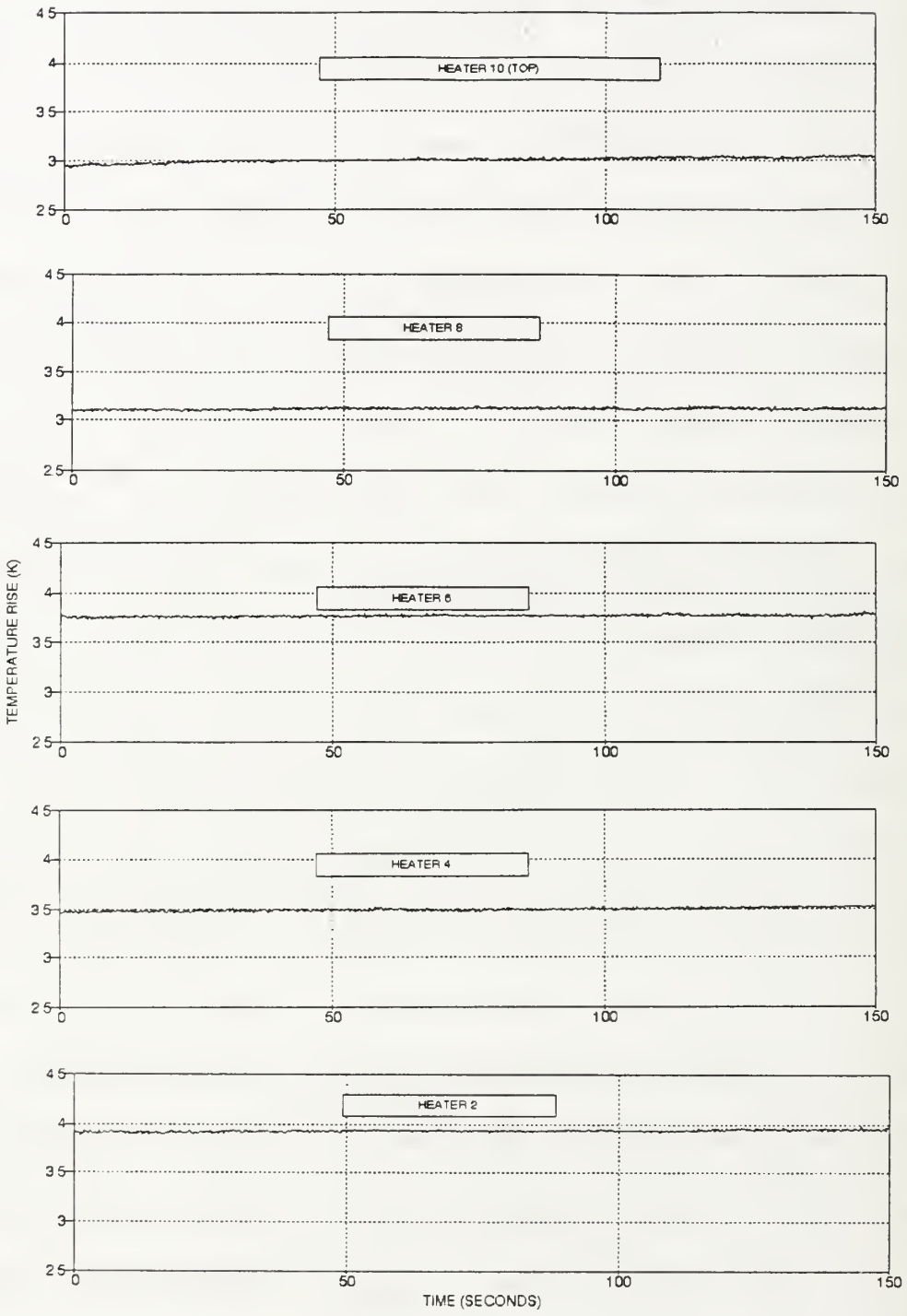

Figure 24. Temperature Rise versus Time. Heat flux= $1050 W/m^2$; Re=4000.

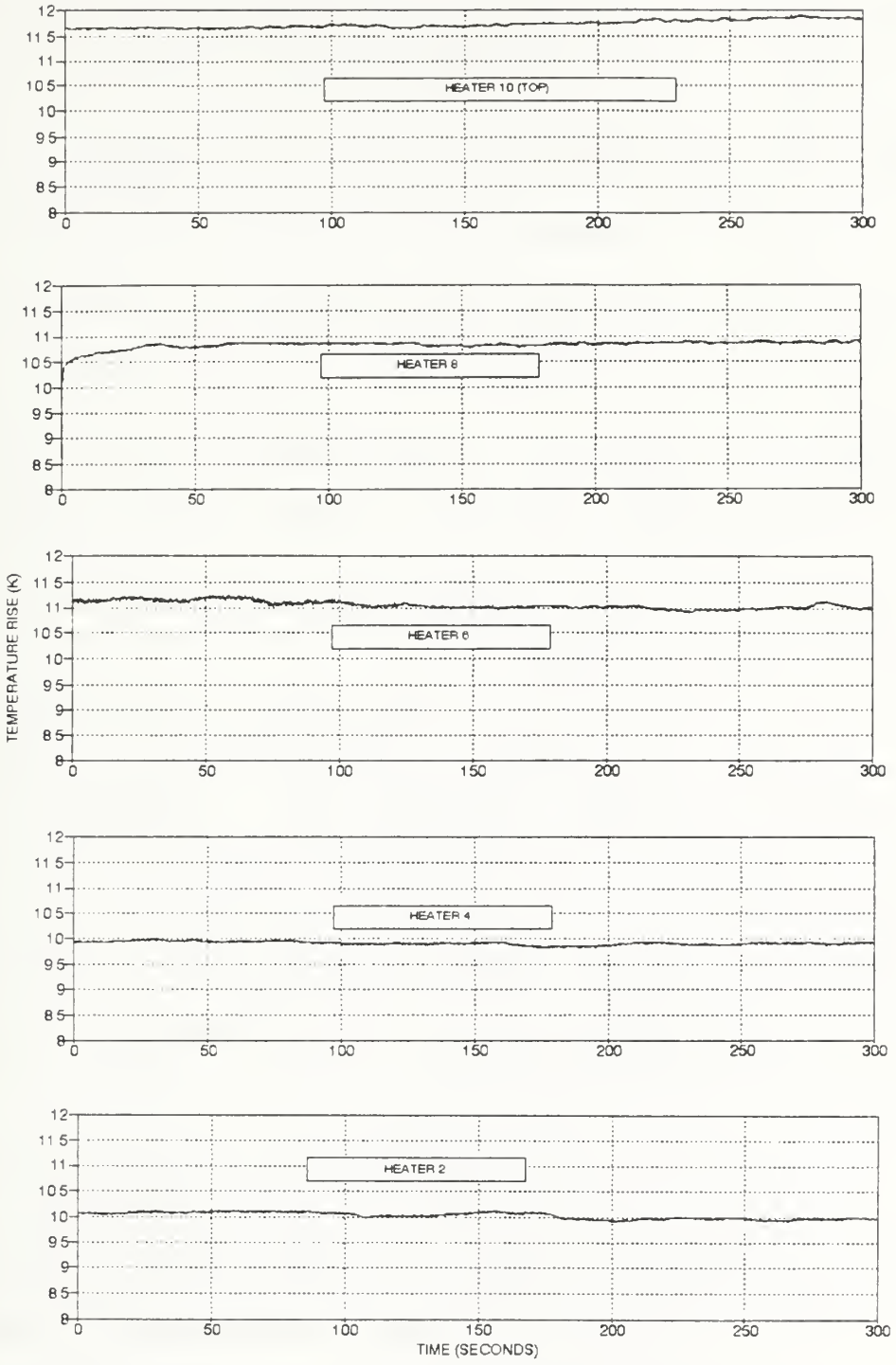

Figure 25. Temperature Rise versus Time. Heat flux= $2505 W/m^2$; Re=500.

natural convection clearly dominating despite only five of ten heaters being powered. In addition, no timewise fluctuation in temperature was observed on any of the heaters.

The Reynolds number was then increased to 1000 and the results are shown in Figure 26. Timewise fluctuations in temperature rise have reappeared and are similar to those observed for the case of all heaters powered. Figure 27 shows results for Re=2000. Timewise fluctuations in temperature rise are still present; however, the period of fluctuation appears to have shortened.

Finally, the Reynolds number was increased to 4000 and the results are shown in Figure 28. Although, forced convection appears to be dominating, no definite trend is observed in the heater temperature rises in the downstream direction. Timewise fluctuations have disappeared on all the heaters.

In conclusion, the top portion of Figure 29 shows Average Nu versus Re for the top heater (HS10). It is seen that Nu for the highest heat flux is substantially below the other heat fluxes for the same Reynolds number. In addition, theoretical values for a constant heat flux condition in a

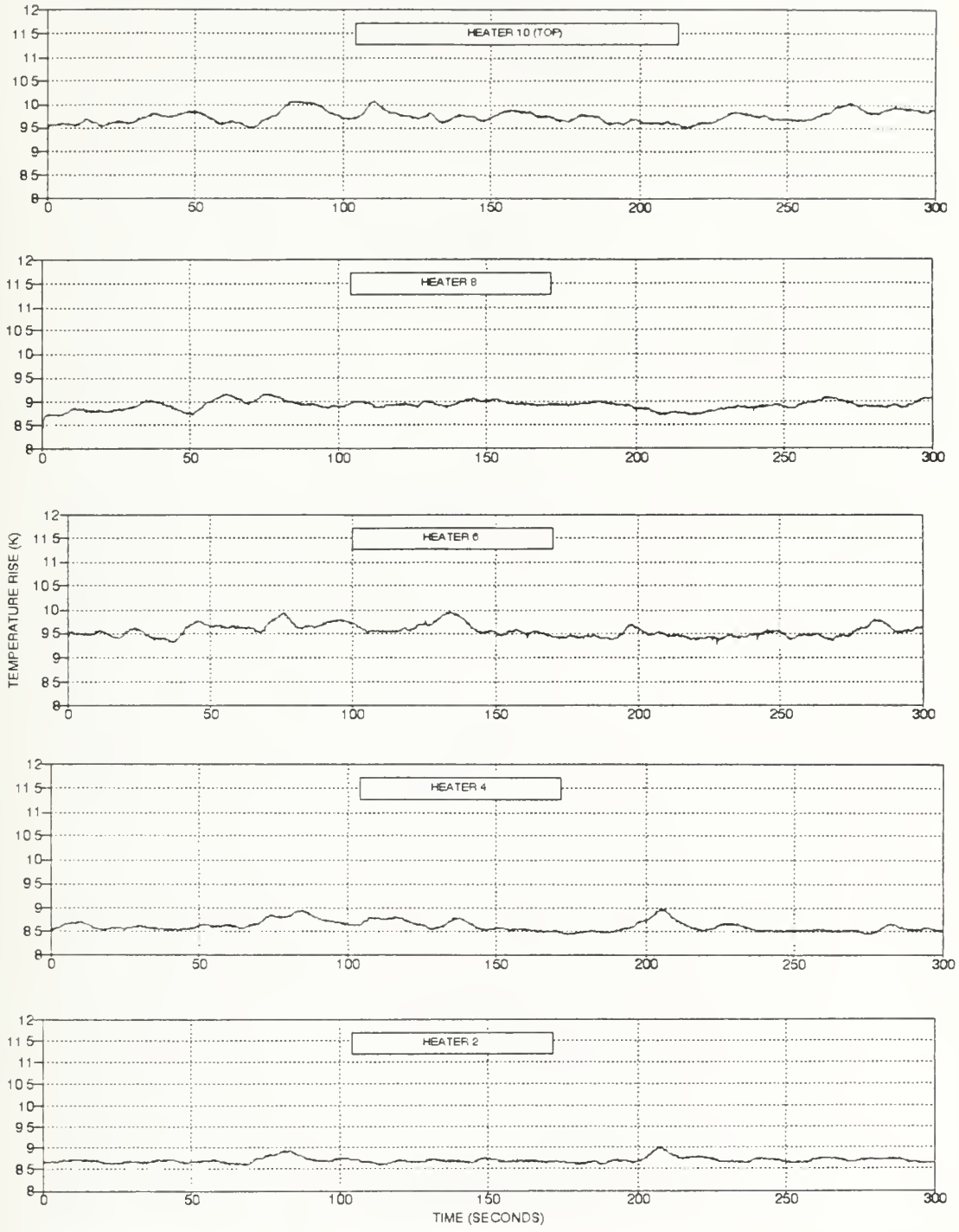

Figure 26. Temperature Rise versus Time. Heat flux= $2505 W/m^2$; Re=1000.

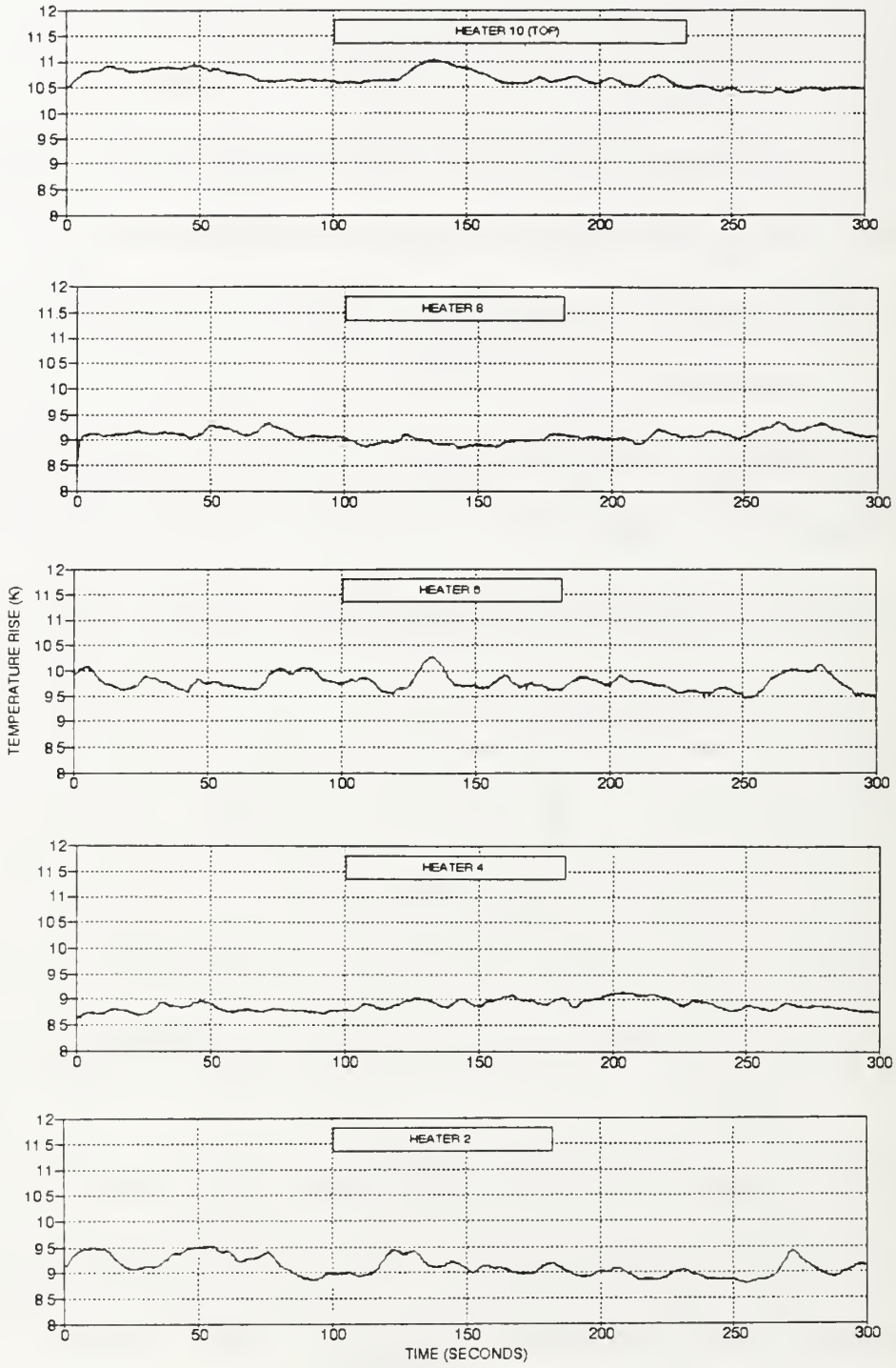

Figure 27. Temperature Rise versus Time. Heat flux= $2505 W/m^2$; Re=2000.

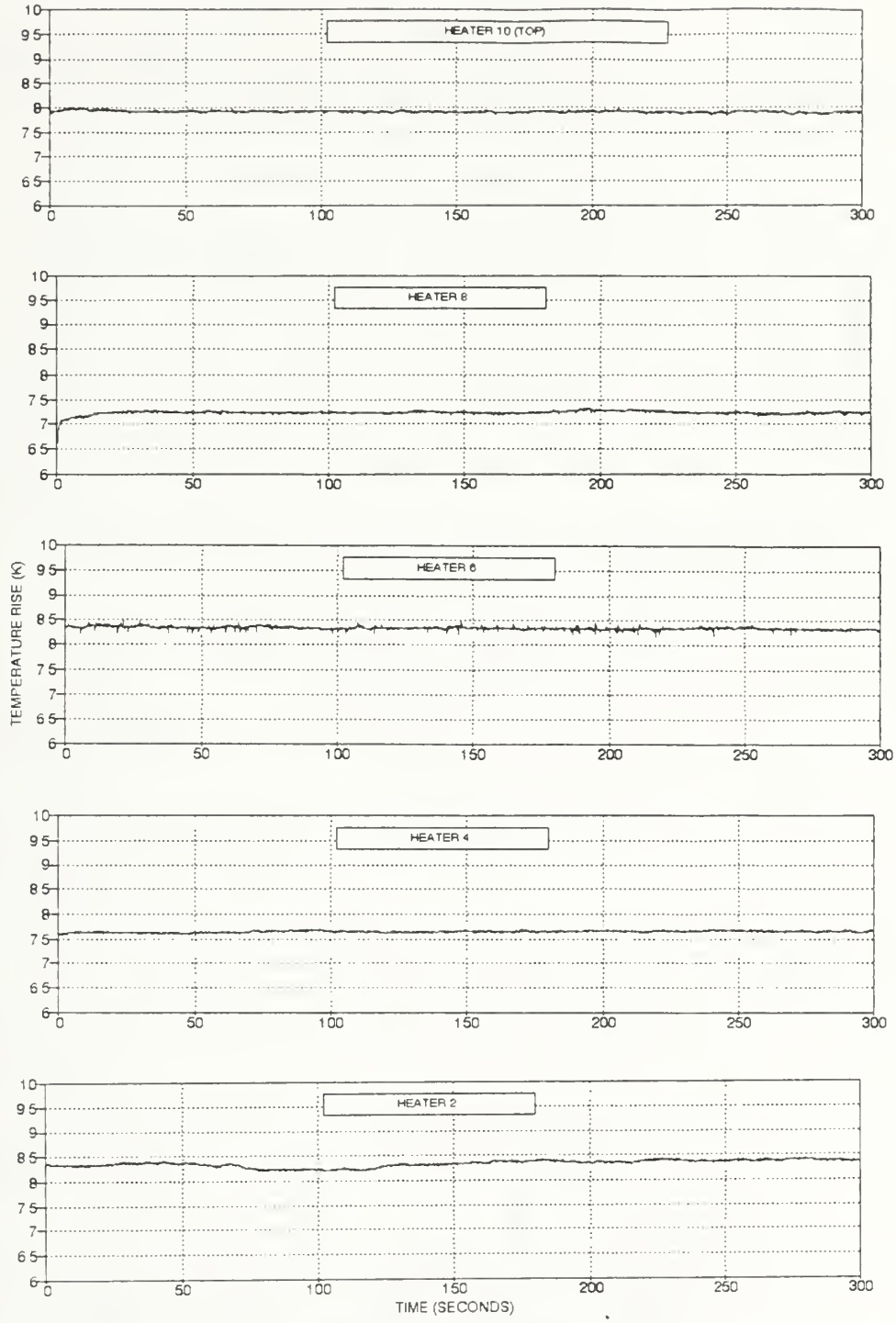

Figure 28. Temperature Rise versus Time. Heat flux= $2505 W/m^2$; Re=4000.

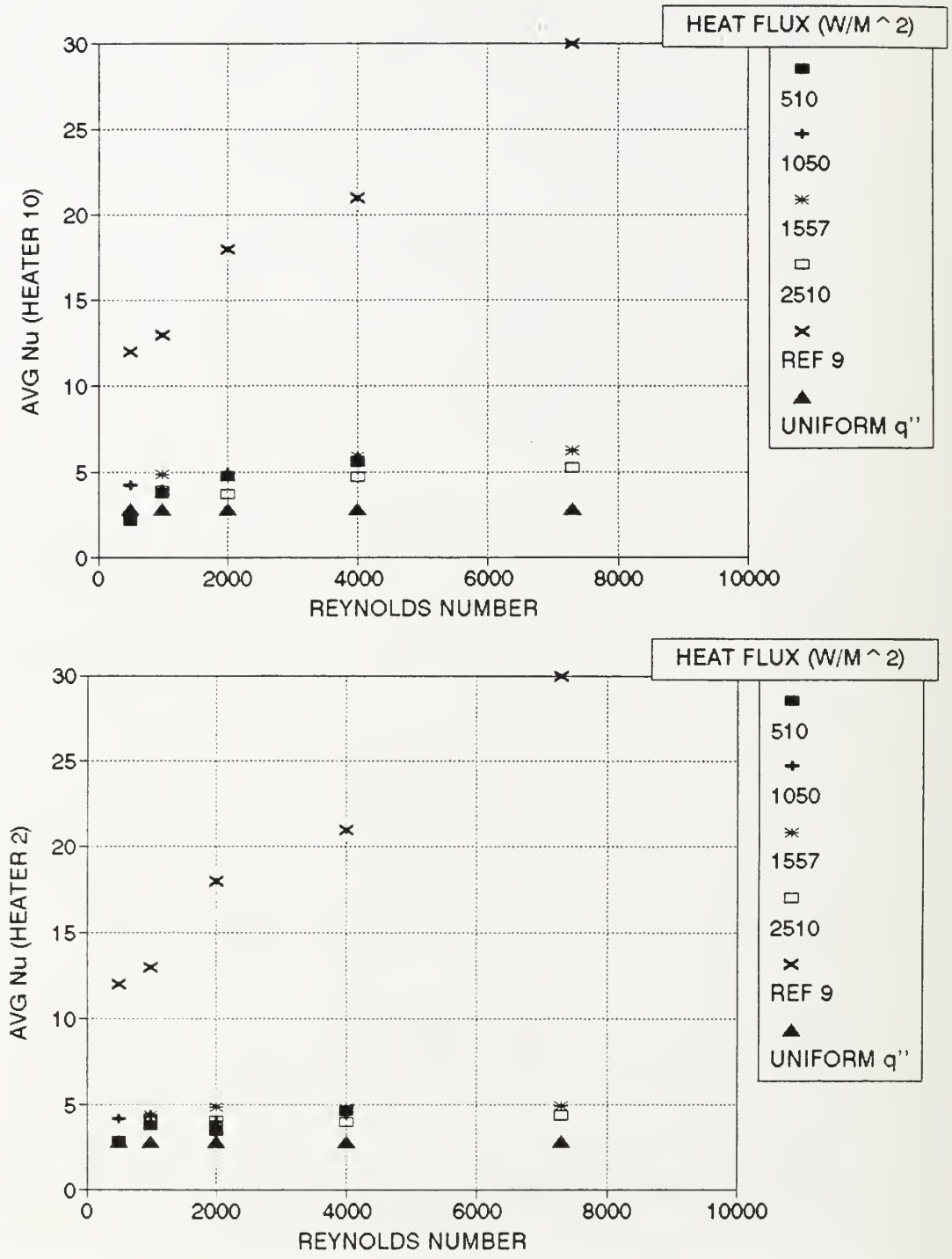

Figure 29. Average Nusselt number versus Reynolds number.

Heater 10(top); Heater 2(bottom).

semi-infinite rectangular channel and values from Incropera (Reference 9) for discrete heat sources in a vertical channel are also shown. The values from Reference 9 are substantially higher than those obtained in the present study. The study in Reference 9 utilized much smaller heaters and it is clearly evident that Nu is highly area dependent. The highest heat flux is producing the most pronounced mixed convection and the buoyancy effects are the greatest at the top heater. The lower portion of figure 29 shows the same results for a bottom heater, heater 2. It is seen that the Nu for the various heat fluxes are closer to each other . The cumulative buoyancy effects are not as great at the lower heaters.

2. Transient Results

All transient data were taken for $q''=2500 W/m^2$ and Reynolds number of 1000.

Figures 30(a)-(e) show transient temperature response with all heaters powered for heaters 10,8,6,4 and 2, respectively. Figure 30(a), displaying results for heater 10, shows that timewise fluctuations begin after about 25 seconds following a sudden powering of all heaters. The temperature rise achieves a nominally steady value of about $10°C$ after

about 200 seconds and oscillates around it. This was expected as Figure 17 showed temperature fluctuations for all heaters powered. The response for heater 8, Figure 30(b), displays the temperature rise beginning to oscillate after 45 seconds. Responses for heaters 6,4 and 2, Figures 30(c)-(e), all indicate a fluctuation in temperature rise beginning after 25 seconds.

Next, every alternate heater was powered and temperature measurements were taken by the center thermocouple on the powered heaters (HS10,8,6,4,2) with the results shown in Figures 31(a)-(e) respectively. All figures show the temperature oscillations begin after about 50 seconds on all heaters. Temperature measurements during this run were also taken on heater 9, an unpowered heater. The results are shown in Figure 32. They show the fluctuations begin after about 65 seconds.

Finally, temperature measurements were taken on heaters 7,6 and 5 with only heater 6 powered. The results are shown in Figure 33. Heater 6 displays temperature fluctuations after about 30 seconds. The adjacent unheated

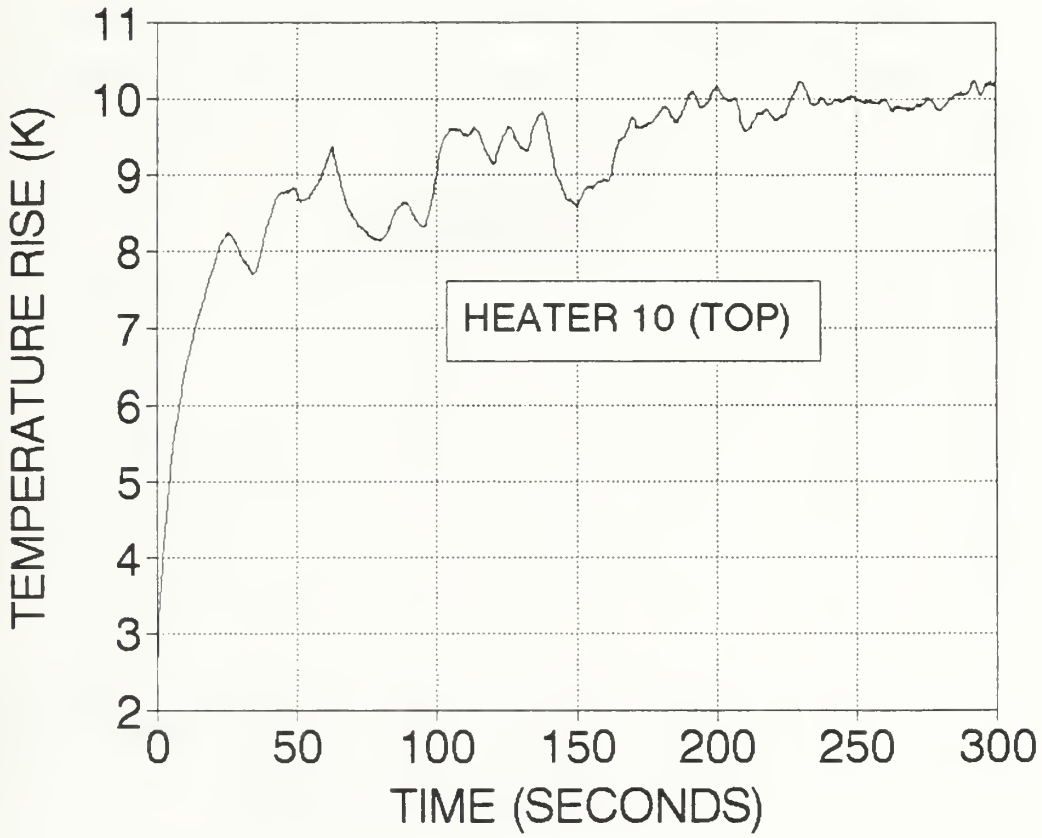

Figure 30(a). Transient Temperature Rise versus Time.

Heat flux= 2500W/m^2 ; Re=1000.

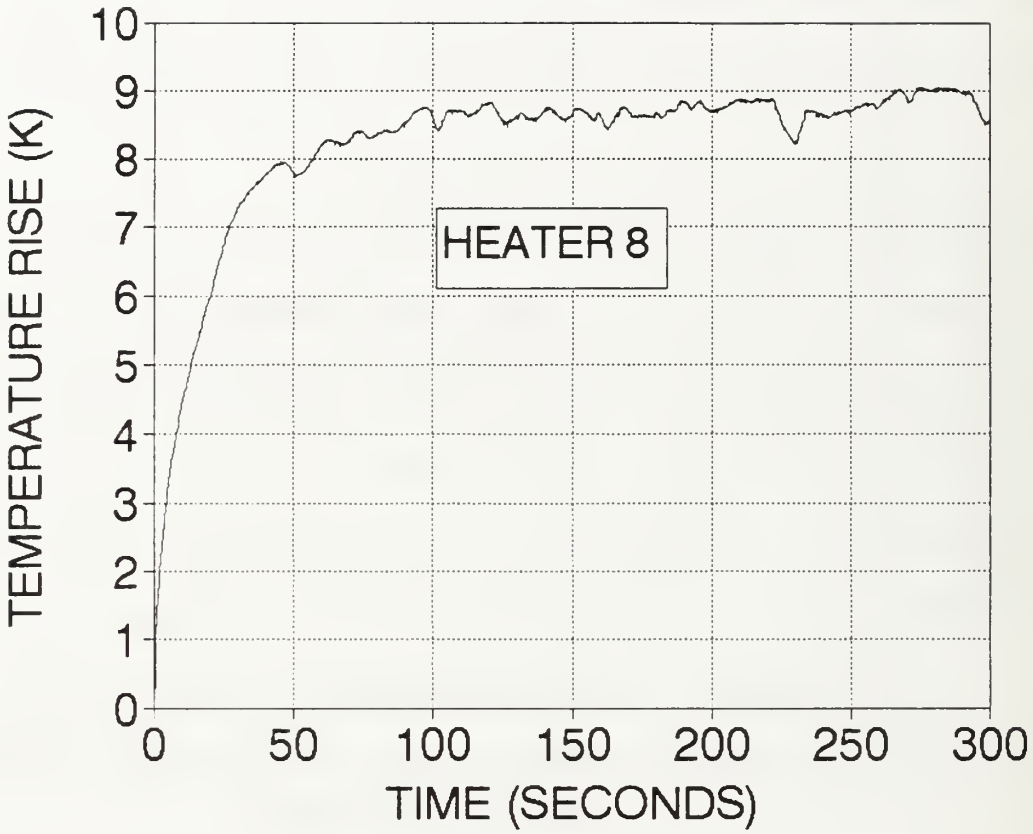

Figure 30(b). Transient Temperature Rise versus Time.

Heat flux= 2500W/m^2 ; Re=1000.

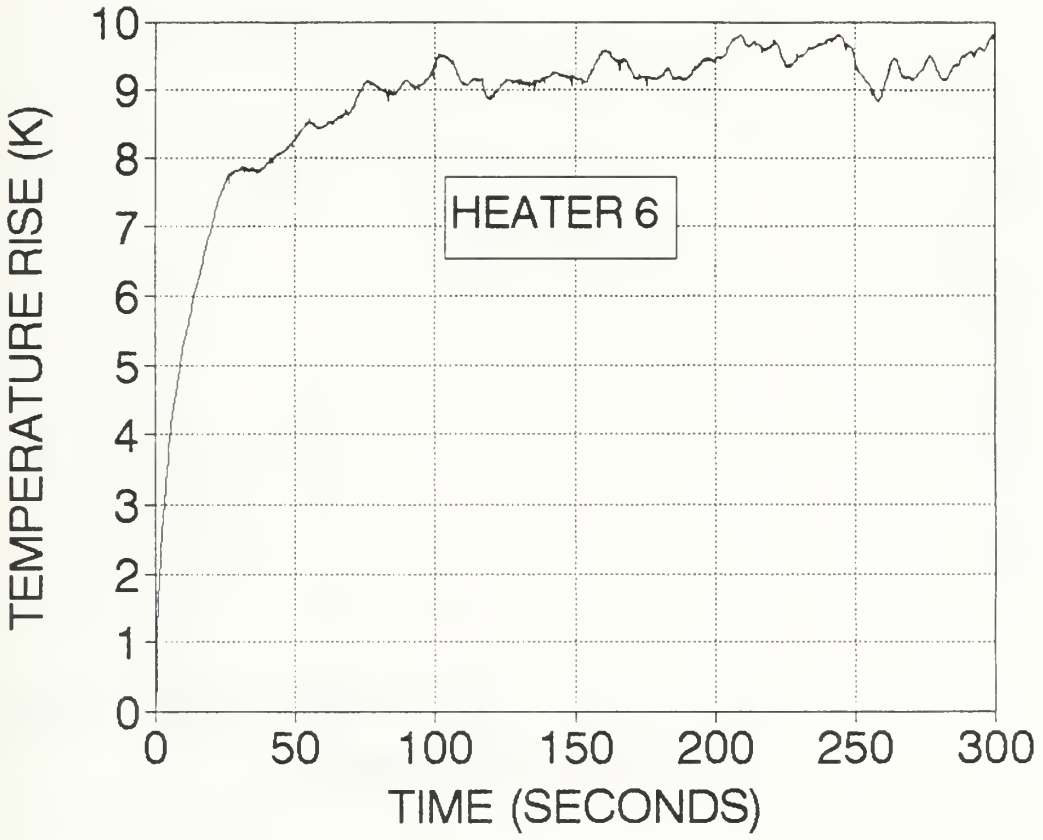

Figure 30(c). Transient Temperature Rise versus Time.

Heat flux= 2500W/m^2 ; Re=1000.

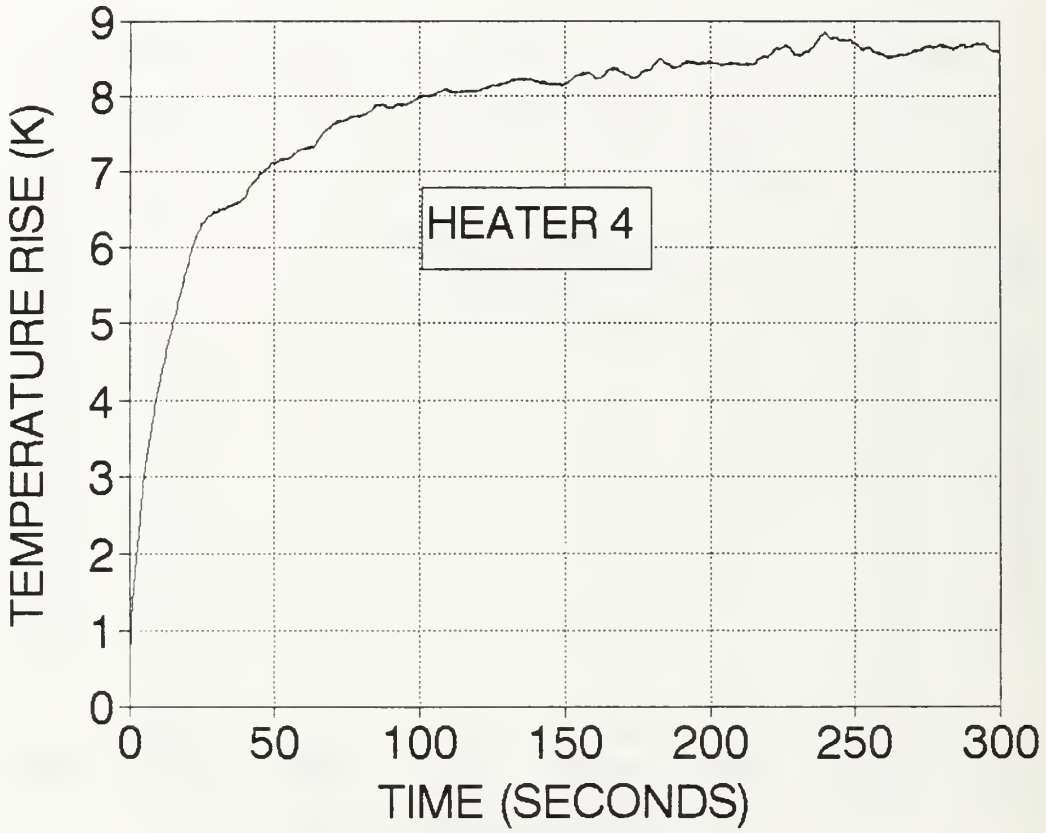

Figure 30(d). Transient Temperature Rise versus Time.

Heat flux= 2500W/m^2 ; Re=1000.

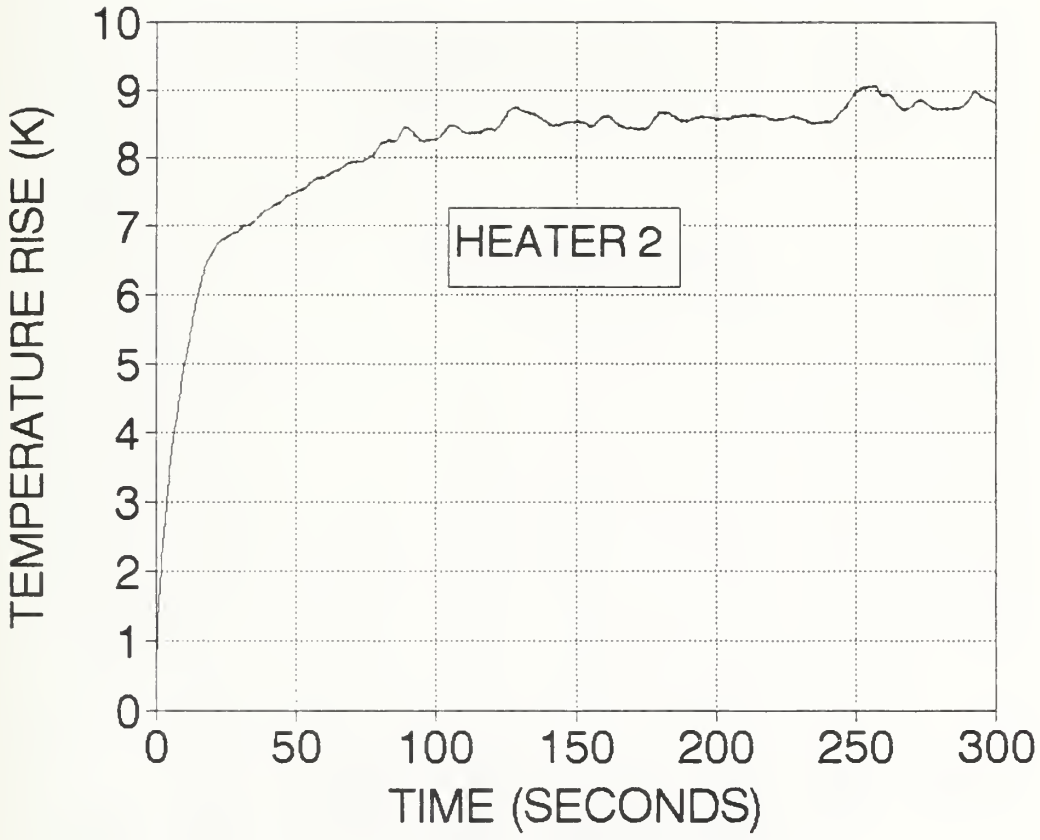

Figure 30(e). Transient Temperature Rise versus Time.

Heat flux= 2500W/m^2 ; Re=1000.

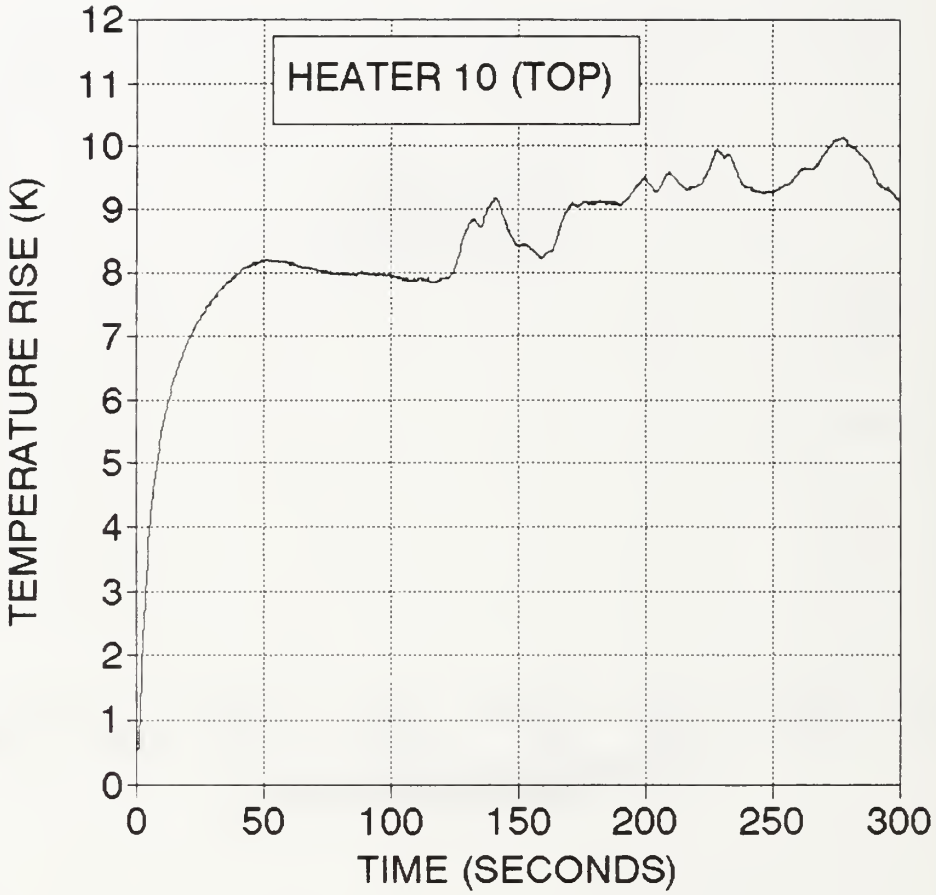

Figure 31(a). Transient Temperature Rise versus Time.

Heat flux= 2500W/m^2 ; Re=1000.

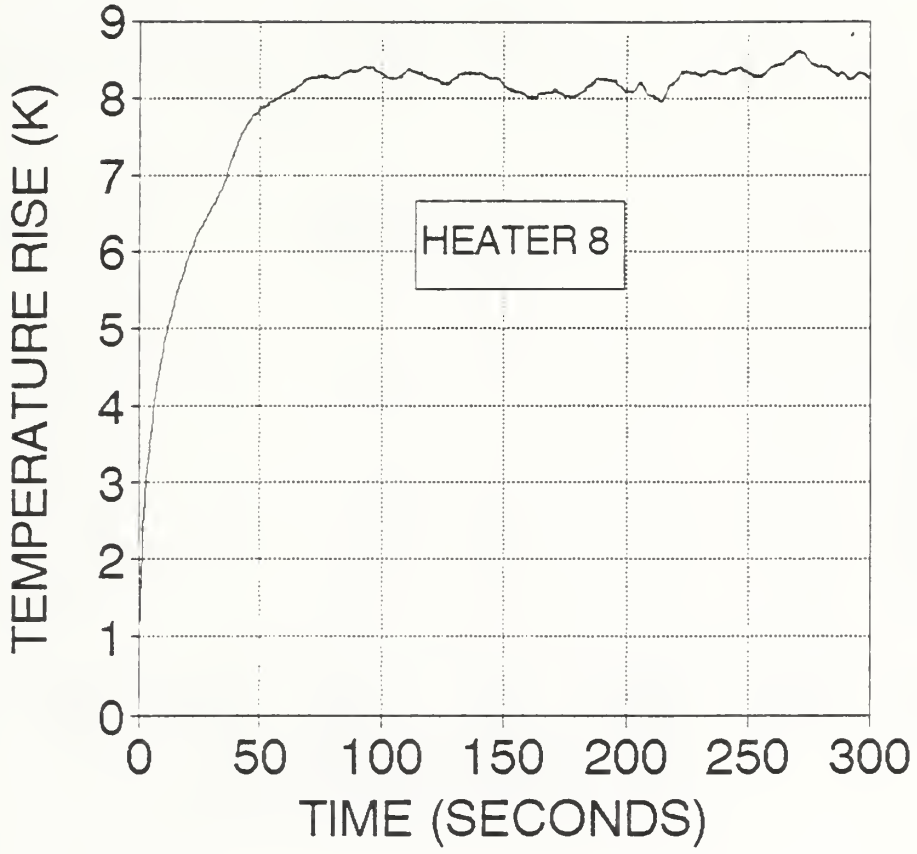

Figure 31(b). Transient Temperature Rise versus Time.

Heat flux= 2500W/m^2 ; Re=1000.

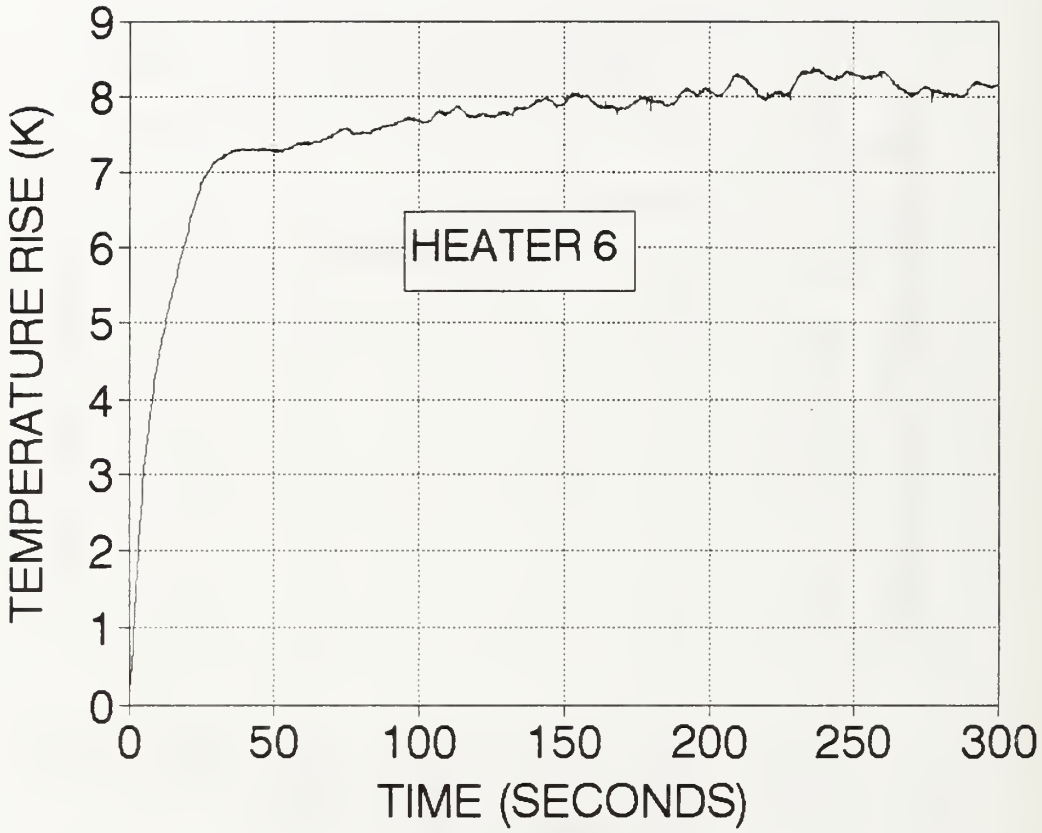

Figure 31(c). Transient Temperature Rise versus Time.

Heat flux= 2500W/m^2 ; Re=1000.

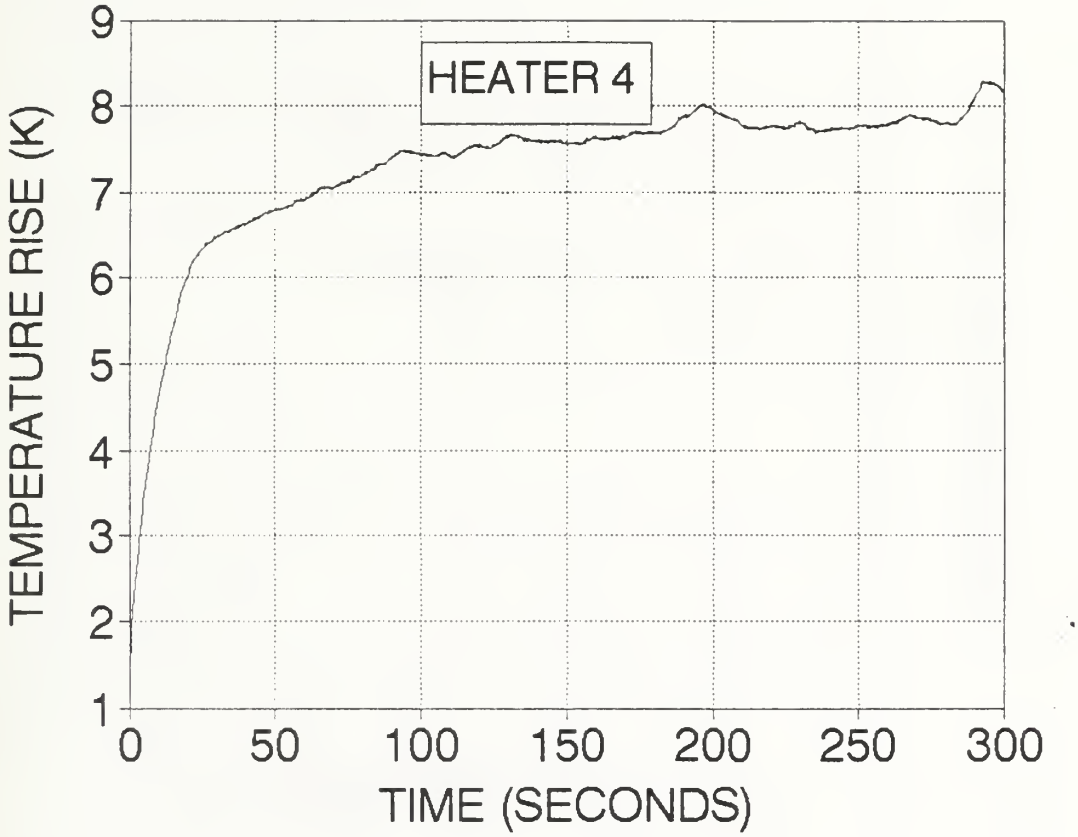

Figure 31(d). Transient Temperature Rise versus Time.

Heat flux= 2500W/m^2 ; Re=1000.

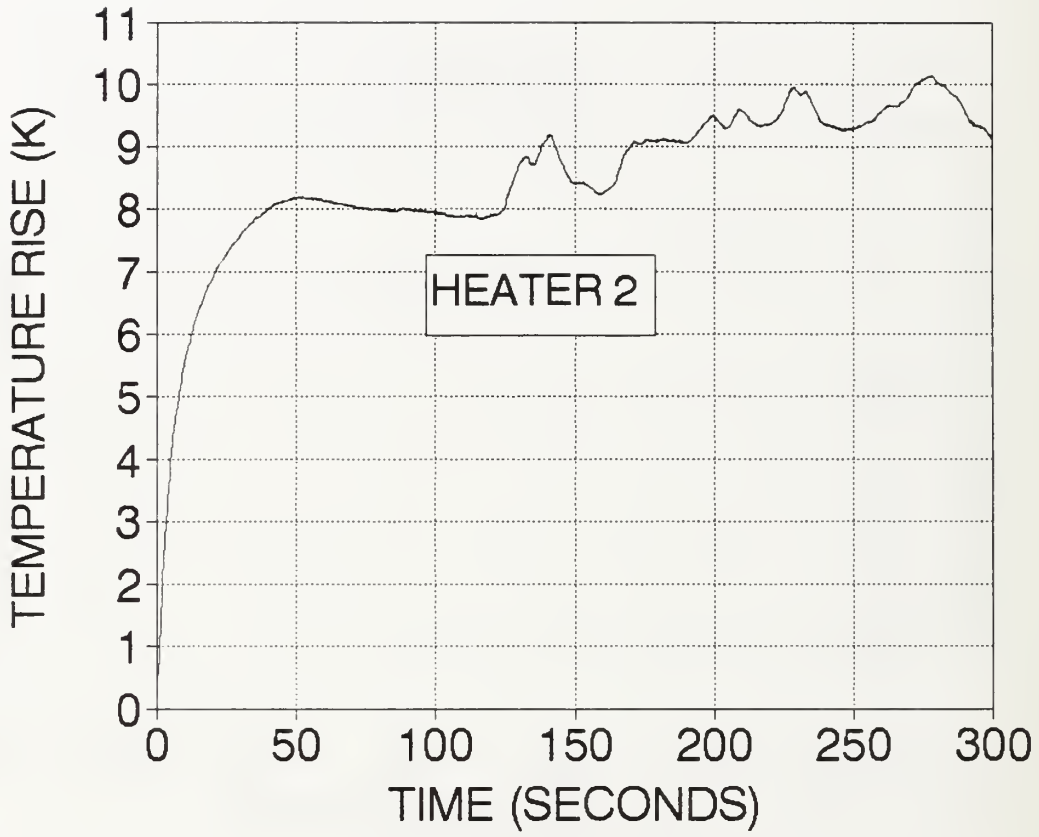

Figure 31(e). Transient Temperature Rise versus Time.

Heat flux= 2500W/m^2 ; Re=1000.

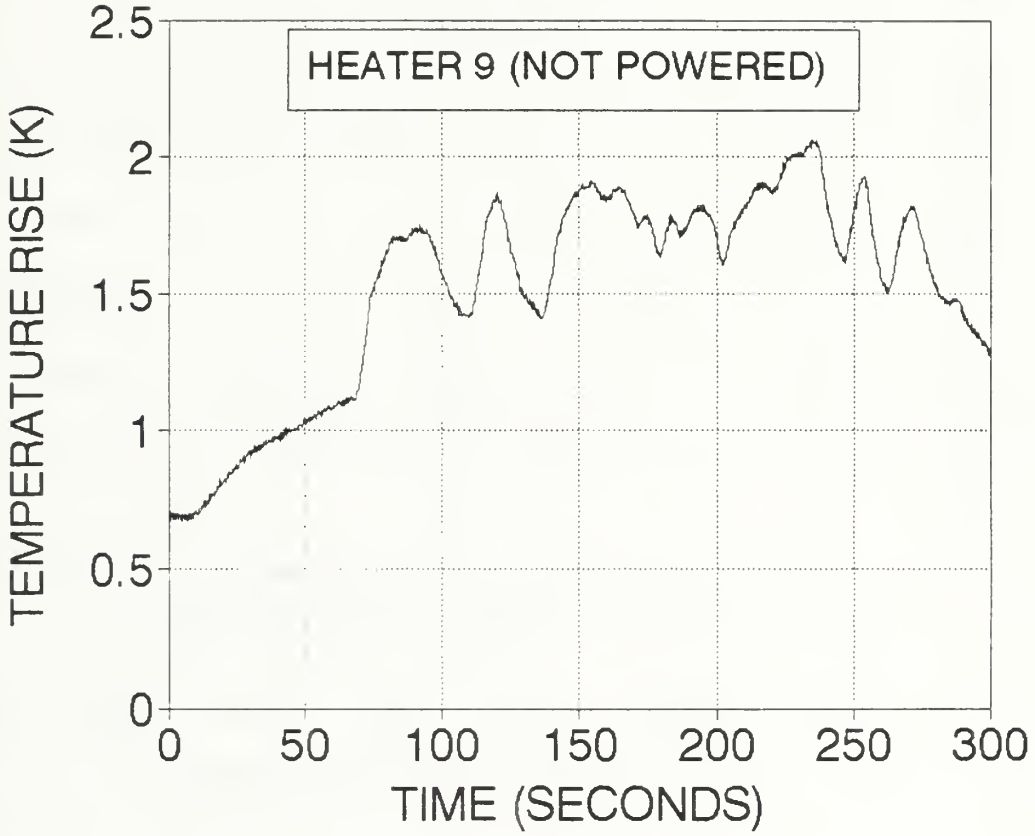

Figure 32. Transient Temperature Rise versus Time.

Heat flux= 2500W/m^2 ; Re=1000.

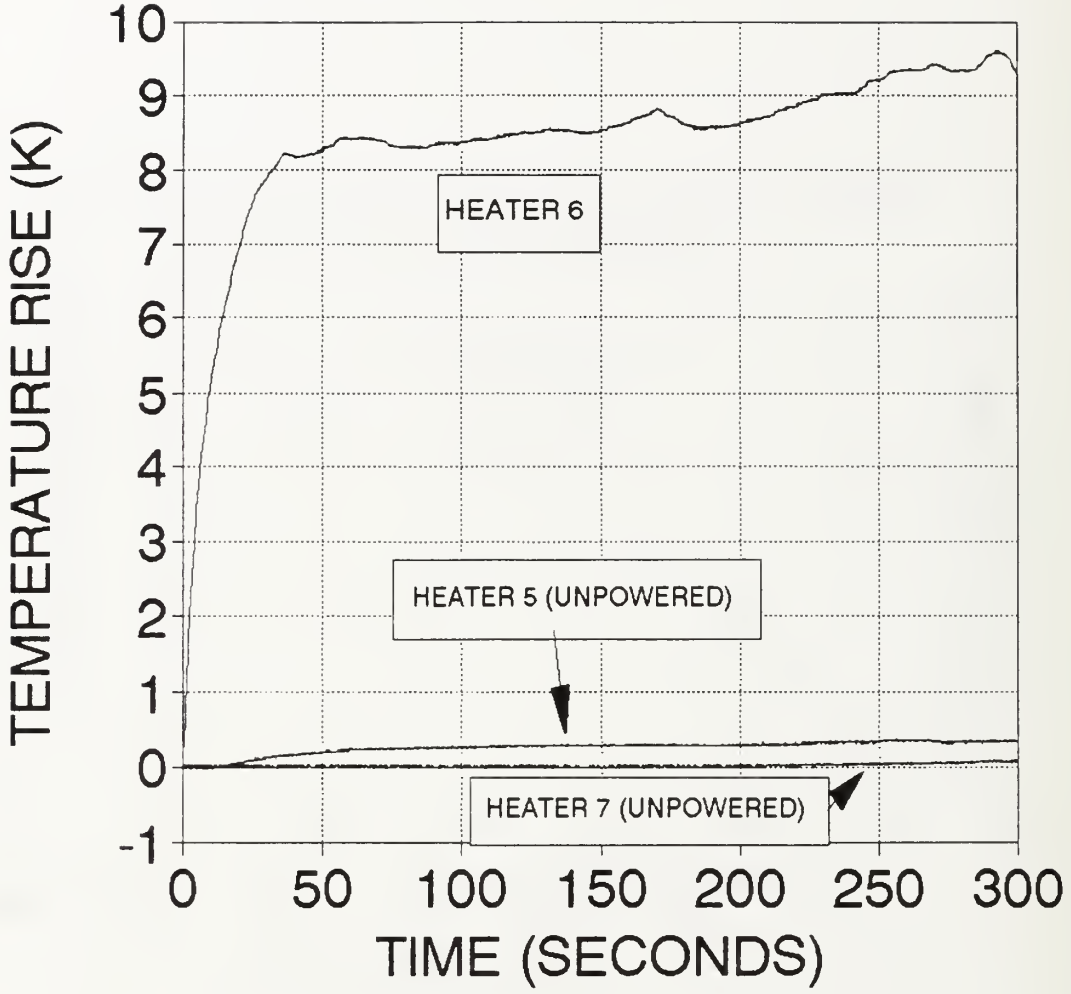

Figure 33. Transient Temperature Rise versus Time.

Heat flux= 2500W/m^2 ; Re=1000.

heaters display only small temperature rises and negligible fluctuations.

D. LIQUID CRYSTAL RESULTS

During the course of taking the mixed convection data, the surface temperature patterns were also visualized using a liquid crystal sheet with a color start temperature of $30°C$. At this temperature the sheet began to turn yellow. Shades of green and blue were observed over approximately a $5°C$ bandwidth.

As shown in Figure 34, at low Reynolds numbers (<2000) and a high heat flux ($q''=2505 W/m^2$), the crystals displayed dark blue bands at the heater locations implying temperatures at or above $35°C$. An interesting phenomenon was observed on the top two heaters. There were buoyant plumes originating at discrete spanwise locations along the heater strips and extending vertically above the strips. Each plume was about 1 cm wide and 3 cm high. These plumes were almost equally spaced about 2 cm apart and were greenish-blue in color. The plumes were directly above one another on heaters 9 and 10. Below those heaters, a milky white appearance was seen below the visualized plumes on heaters 9 and 10. These milky white

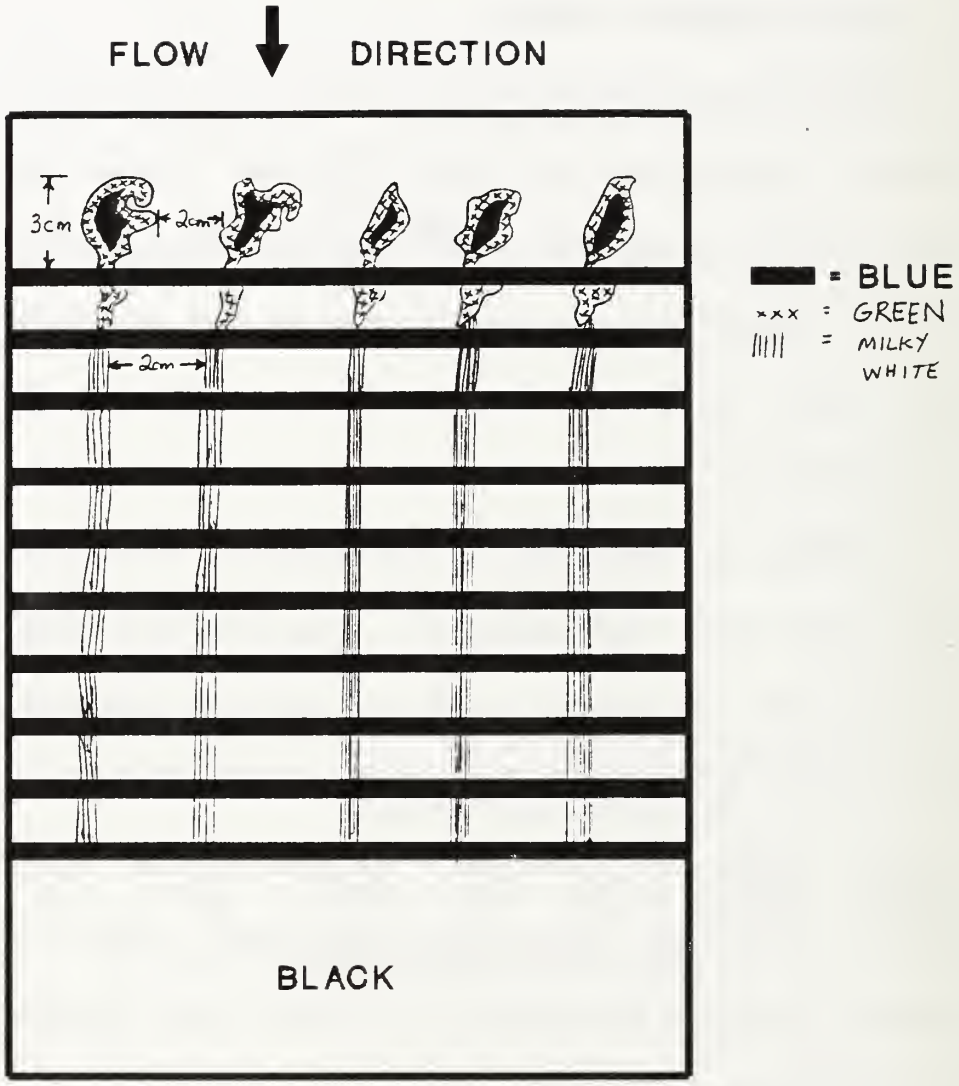

Figure 34. Liquid Crystal Sheet appearance. Heat flux= $q''=2505 W/m^2$; Re=2000.

streaks extended all the way down the liquid crystal sheet. The liquid crystal sheet was initially black, so there seemed to be some temperature rise of the area between the lower heaters. The same results were obtained, to a lesser degree, for lower heat fluxes.

IV. CONCLUSIONS

During the course of this study, several conclusions were reached about opposed mixed convection heat transfer from discrete heat sources in a vertical channel.

The pulsatile flow study was inconclusive. It is still not clear whether oscillating the flow helps or hurts heat transfer. In some cases it was seen that oscillation seemed to be helping; however, the enhancement cases barely fell outside the uncertainty band. It was not possible to ascertain the amplitude of flow pulsations in the test section due to the downstream vane. Laser Doppler Velocimeter measurements must be taken to ascertain these.

The second part of the experimental study examined the effects of opposed mixed convection with no vane rotation. The main finding in this part of the investigation was that for low Reynolds numbers and sufficiently high heat fluxes a strong opposed mixed convection environment is present in the vertical channel.

This opposed mixed convection environment causes very large surface temperature fluctuations on the heating strips.

This is highly undesirable as cyclic temperature fluctuations in electronic components would severely degrade the operating life of that component. Thus, avoiding flow rates (Re<2000 for a vertical channel) which lead to a strong opposed mixed convection regime are highly recommended.

V. RECOMMENDATIONS

In continuation of this study it is recommended that follow on studies include:

- Velocity field determination using a Laser Doppler Velocimeter
- Investigation of aiding mixed convection by reversing the forced flow inlet and outlet locations.
- Development of a numerical model to predict the effects of opposed mixed convection in a vertical channel.

APPENDIX A

UNCERTAINTY ANALYSIS

In order to ascertain the accuracy of the quantities obtained from data reduction, it was necessary to complete an uncertainty analysis. The values measured during the course of the experimental program included; power input, thermocouple outputs, and length of the heaters and channel. The accuracy of these values were ± 0.001 Watt for power, ± 0.20 $^{\circ}C$ for temperature difference and ± .05 mm for lengths. The estimates for the measured quantities were used in calculation of the uncertainty of necessary non-dimensional quantities.

Reference 10 provided the basis for the uncertainty analysis. The uncertainty of a particular variable R which is a function of several variables V:

$$R=R(V_1, V_2, \ldots, V_n)$$

can be determined by using the expression:

$$\delta R=[((\frac{\partial R}{\partial V_1})\delta V_1)^2+((\frac{\partial R}{\partial V_2})\delta V_2)^2+((\frac{\partial R}{\partial V_n})\delta V_n)^2]^{\frac{1}{2}}$$

δ Pwr, δ L, $\delta\Delta$ T, were defined as the uncertainty for power, length and temperature difference respectively. The uncertainty of the value for Nu was computed as follows:

$$\delta Nu=\frac{1}{K_f}[(L\delta h)^2+(h\delta L)^2]^{\frac{1}{2}}$$

where δ h is given by:

$$\delta h=[(\frac{1}{A_s\Delta T})\delta Pwr)^2+((\frac{Pwr}{A_s(\Delta T)^2})\delta\Delta T)^2+((\frac{Pwr}{\Delta T(A_s)^2})\delta(A_s))^2]^{\frac{1}{2}}$$

The above equations produced a maximum uncertainty for Nu of $\pm$ 0.07 for a nominal value of Nu=3.59.

The above procedure was used to determine the uncertainties in Gr^*, and Re. Without listing the equations, the maximum uncertainty for Gr^* was 3042 for a nominal value 189,301. The maximum uncertainty for Re was 10 for a nominal value of 2000.

APPENDIX B

SAMPLE CALCULATIONS

The following calculations are based on the average temperature of a single heater measured in the center of the channel, over a time span of five minutes, on heater 10 and with a heat flux of 2505 W/m^2 and a Reynolds number of 2000 with no vane rotation. The average Δ T was 11.27 $^{\circ}C$.

1. CHARACTERISTIC DIMENSIONS

Perimeter (P) = 2(0.2+0.01)

= 0.42 m

Heater surface area (A_s) = (0.20)(0.01)

= .002 m^2

Channel cross sectional area (A_c) = (0.20)(0.01)

= .002 m^2

Hydraulic diameter (D_h) = 4(0.002)/0.42

= 0.019 m

2. CONVECTIVE HEAT FLUX

Power to heater (Q_{conv}) = 5.01 W

Heat flux (q'') = 5.01/.002

= 2505 W/m^2

3. WATER PROPERTIES [REF.8]

Film temperature (T_{film}) = (25.0+36.27)/2 + 273.15

= 303.8 K

β = 306E-6 1/K

ν = 0.802E-6 $\frac{m^2}{sec}$

k_f = 0.618 W/m K

4. REYNOLDS NUMBER

Re = (0.0844)(0.0190)/(.802E-6)

= 2000

5. HEAT TRANSFER COEFFICIENT

h = 2505/11.27

= 222 W/m^2K

6. NUSSELT NUMBER

Nu = (222.27)(.01)/(0.618)

= 3.59

7. FLUX BASED GRASHOF NUMBER

Gr^* = (9.81)(306E-6)(2505)(.01^4)/(.618)(.802E-6^2)

= 189,173

LIST OF REFERENCES

1. Bar-Cohen, A., and Kraus, A.D., *Advances in Thermal Modeling of Electronic Components and Systems*, ASME Press, 1990.

2. Chu, R.C., "Heat Transfer in Electronic Systems," *The 8th International Heat Transfer Conference Proceedings*, v.I, 1986.

3. Lemlich, R., "Vibration and Pulsation Boost Heat Transfer," *Chemical Engineering*, v.68, pp. 171-174, 15 May 1961.

4. Azar, K., "Effect of Forced Oscillation at the Channel Entrance for Enhanced Cooling of Components in Electronic Circuit Pack Channels," AIAA/ASME 5th Joint Thermophysics and Heat Transfer Conference, June 18-20, 1990.

5. Siegel, R., and Perlmutter, M., "Heat Transfer for Pulsating Laminar Duct Flow," *Journal of Heat Transfer*, v.84, pp. 111-123, May 1962.

6. Ludlow, J.C., Kirwan, D.J., and Gainer, J.L., "Heat Transfer with Pulsating Flow," *Chemical Engineering Communicum*, V.7, pp.211-218, 5 Aug 1980.

7. Gebhart, B., Jaluria, Y., Mahajan, R.L. and Sammakia, B., *Buoyancy Induced Flows and Transport*, Hemisphere Publishing, 1988.

8. Incropera, F.P., and Dewitt, D.P., *Introduction to Heat Transfer*, John Wiley & Sons, Inc., 1985.

9. Incropera, F.P., et al, 1986, "Convection Heat Transfer From Discrete Sources in a Rectangular Channel," *International Journal of Heat and Mass Transfer*, Vol. 29, pp. 1051-1058.

10. Kline, S.J., and McClintock, F.A., "Describing Uncertainties in Single Sample Experiments," *Mechanical Engineering*, January, 1953.

INITIAL DISTRIBUTION LIST

		Copies
1.	Defense Technical Information Center Cameron Station Alexandria, Virginia 22304-6145	2
2.	Library, Code 0142 Naval Postgraduate School Monterey, California 93943-5002	2
3.	Prof. A.J. Healey, Code ME/Hy Department of Mechanical Engineering Naval Postgraduate School Monterey, California 93943-5002	1
4.	Prof. Y. Joshi, Code ME/Ji Department of Mechanical Engineering Naval Postgraduate School Monterey, California 93943-5002	2
5.	Mr. Kip Hoffer Naval Weapons Support Center Code 6042 Crane, Indiana 47522	1
6.	Mr. Tony Buechler Naval Weapons Support Center Code 6042 Crane, Indiana 47522	1
7.	Naval Engineering Curricular Office, Code 34 Naval Postgraduate School Monterey, California 93943-5002	1
8.	James D. Syring 3204 Woodbridge Ave. Muncie, Indiana 47304	1

Thesis
S966 Syring
c.1 Mixed and forced convection from an array of discrete heat sources in a vertical channel.

Thesis
S966 Syring
c.1 Mixed and forced convection from an array of discrete heat sources in a vertical channel.

AMERICAN BINDERY
10-93

DUDLEY KNOX LIBRARY
3 2768 00036294 1